CHAPTER 2

Synthesis and characterization of bioactive ligands

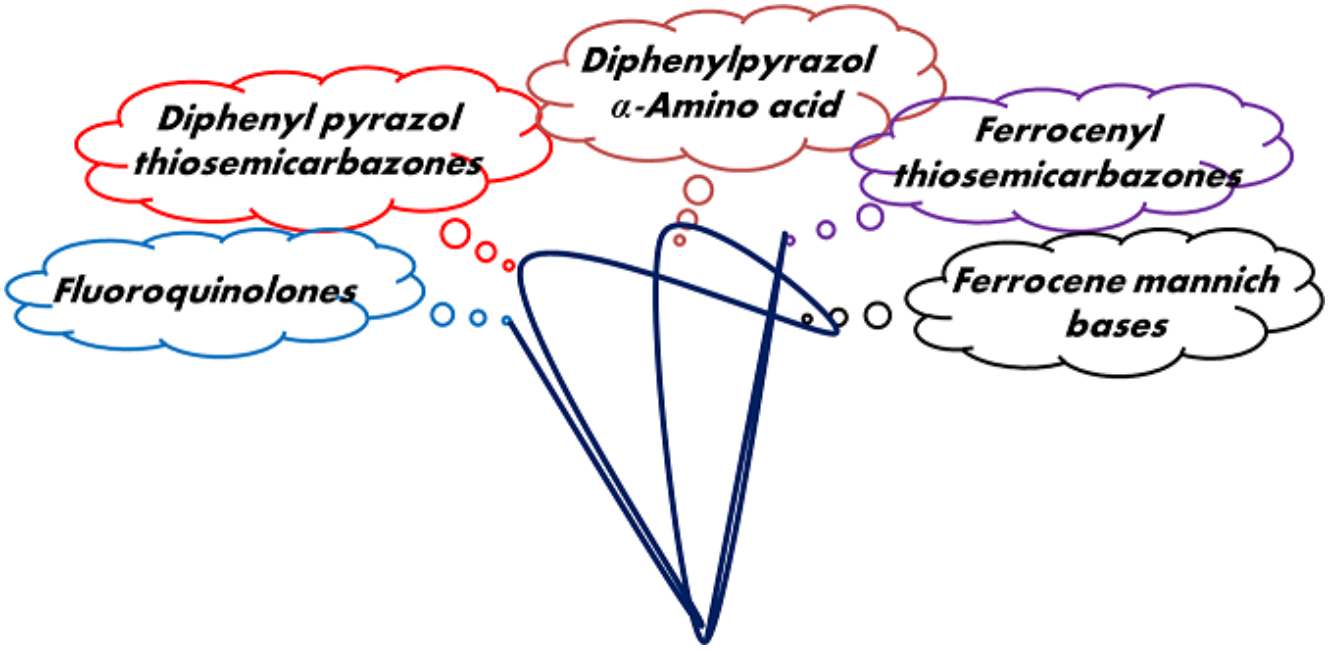

This chapter focuses on the synthesis and characterization of a selected range of five different organic compound series whose bioactivities are well established and have hetero-atoms (N, O, and S) as coordination sites to the ruthenium (II) centre in order to design good biologically active metal complexes with an aim to study their potential as anticancer agents. These ligands have been synthesized and well characterized by Mass spectrometry, NMR, FTIR and UV-Vis spectroscopy.

TABLE OF CONTENTS

2.1 Chemistry and Biological Importance of Heterocyclic moiety:

2.1.1 Important features of Heterocyclic Compounds:

Heterocycles are commonly seen in many biological systems, occurring in a wide range of structures from enzyme co-factors through to amino acids and proteins. They play an important role in the metabolism of all living organisms, and are utilised at almost all stage of biochemical processes necessary to sustain life. The heterocyclic bases-pyrimidines and purines are constituents of the genetic material DNA. A large number of synthetic and natural heterocyclic compounds are pharmacologically active and are in clinical use.

According to statistics, more than 85% of all biologically-active compounds contain a heterocycle. Heterocycles play major roles in modern drug design providing useful tools for variation in solubility, lipophilicity, polarity, and hydrogen bonding capacity of biologically active agents, which leads to the optimization of the ADME properties of the drugs or drug candidates. Many heterocyclic lead compounds were isolated from natural resources, and their structures modified by medicinal chemists. Thus, heterocycles are important for medicinal chemists, because using them; they can broaden the available drug-like molecules and run more effective drug discovery programs [1]

The role of heterocycles in anti-cancer drug design:

Heterocycles are key structural components of many of the anti-cancer drugs marketed today. Their prevalence in anti-cancer drug design is partially attributed to their being widely found in nature with a number of cellular processes and mechanisms having evolved to interact with them. There are multiple metabolic pathways and cellular processes within cancer pathology that are influenced by heterocycle-based drugs.

As many enzyme binding pockets are predisposed to interacting with heterocyclic moieties, heterocycles are good options for designing molecules that will interact with targets and interupt the mechanism associated with cancer progression. Pathways associated with cell growth are often targeted by such anti-cancer therapies. Moreover, the relative ease by which heterocyclic rings can be modified with additional substituents makes them excellent choice for anti-cancer drug development.

Nitrogen-based heterocycles are of significance in anti-cancer drug design, particularly indoles, as they are able to induce cell death in a number of cancer cell lines [2]. Indole and

its derivatives have been shown to disrupt a number of cellular pathways related to the advancement of cancer. These include cell signalling, cell cycle progression, tumour vascularisation and DNA repair and the ability to induce cellular oxidative stress causing cell death. The indole-based anticancer agents' vincristine and vinblastine known since the 1960s are still clinically used today. The indolocarbazoles exhibit a broad range of activities, and have the received attention in recent years for their anti-cancer properties. Indolocarbazoles can act as protein kinase inhibitors, the enzyme known to play a major role in the malignant transformation of cells during cancer initiation. Midostaurin (an indolocarbazole-based multi-target protein kinase inhibitor), was approved by the FDA for the treatment of acute myeloid leukaemia in April 2017, which demonstrates the relevance of nitrogen-based heterocycles for anti-cancer drug design.

Oxygen-containing heterocycles also feature prominently in many anti-cancer drugs. Paclitaxel, with a oxygen-heterocycle moiety, is a key drug in cancer therapy, causing inhibition of mitosis in cancer cells and retardation of cancer cell division. The oxygen-containing heterocyclic anti-cancer drugs, cabazitaxel and eribulin have been developed lately, to treat prostate and metastatic breast cancer respectively.

Studies related to repurposing of existing oxygen-based heterocyclic drugs originally developed for other diseases, for use as anti-cancer agents are being carried. Auranofin, a heterocyclic compound containing Au, used for the treatment of rheumatic arthritis, is being investigated as a therapeutic agent for the treatment of leukaemia, lymphoma, ovarian (under Phase II clinical trials) and other types of cancer. Repurposing repositioning drugs is an affordable approach to drug discovery, due to the expenditure associated with new molecule identification and other research and development activities [3].

Much like their oxygen- and nitrogen-based counterparts, sulphur-containing heterocycles have received attention in the development of anti-cancer drugs. Thiophene derivatives, known as tyrosine kinase inhibitors, were evaluated for their antiproliferative activity against human breast adenocarcinoma cells, with a number of compounds showing promising inhibitory effects. In addition, a number of thiadiazole and thiazole based heterocycles exhibited anti-cancer activity towards a panel of human cancer cell lines. Dabrafenib, a thiazole-containing anti-cancer drug molecule was approved by the FDA in 2013.2, 6-diamino-substituted purine derivatives as analogues of reversine were synthesized and tested against breast and colorectal cancer cells. The compounds were found to affect the cell cycle

causing cycle arrest in the G2/M phase [4]. Several piperazine derivatives were found to induce apoptosis, decrease the (BCL2/BAX) ratio related to apoptosis regulation, disrupt mitochondrial potential, and suppress the growth of Hela xenografts in nude mice. The compounds showed the IC_{50} values approx. 2 μM on the Hela and MKN45 cell lines [5].

It is clear from these developments that heterocyclic compounds continue to form the basis of a multitude of successful anti-cancer treatments. It is not surprising, therefore, that they continue to be in focus of the medicinal chemists since their vast repertoire of molecular interactions make them excellent candidates for anti-cancer drugs.

The work in this chapter encases the synthesis of four different heterocyclic systems with well-established biological activities.

2.2 Diphenyl pyrazol thiosemicarbazones (L1-L4):

2.2.1 Introduction:

Pyrazoles represent an important pharmacophore with various biological properties, and some pyrazole-containing derivatives have already been used as drugs for therapeutic purposes. Literature reveals that pyrazole derivatives are potent pharmacological compounds, and, therefore, their design and synthesis is an important area of research. The structural modifications of pyrazole, concerning the substituents at the 1-position, the carbon at the 3-position and the substituent at the 5-position have led to the preparation of new derivatives with a broad spectrum of biological activity. Structural modification on the different positions of the basic molecule allows for upgrading its pharmacological profile, providing it with antimicrobial, anticonvulsant, analgesic, anti-inflammatory, anti-viral, anti-malarial and anti-cancer properties. A comprehensive review by A. Ansari et al. focuses on the synthesis of diverse pyrazole derivatives and their biological activities [6]. Several pyrazolo [3,4-d] pyrimidine derivatives possessing antiproliferative activity were reported by Huang et al. [7]. These compounds show antiproliferative activity against a panel of human cancer cell lines, including lung carcinoma (NCl-H226), nasopharyngeal (NPC-TW01), and T-cell leukemia (Jurkat) cells. Mert et al. reported a new series of pyrazole–sulphonamide derivatives that showed antiproliferative activity against HeLa and C6 cell lines [8]. Antiproliferative property of a set of novel benzothiopyranopyrazole derivatives was reported by Via et al. when tested against HeLa and HL-60 cells [9]. The activities were characterized by the

presence of a methoxy substituent at the 7-position and a pendant phenyl, p-chlorophenyl, or p-methoxyphenyl in the 1-position of the heterocyclic moiety, respectively.

The ester and amide derivatives of 1-phenyl-3-(thiophen-3-yl)-1H-pyrazole-4-carboxylic acid exhibited anticancer activities against various cancer cell lines. [10]. Nitulescu et al. synthesized a series of functionally substituted pyrazoles (I–III) (*Fig. 2.1*) and investigated their antiproliferative effects in vitro on a panel of 60 cell lines [11]. Promising results were obtained with N-benzoyl-N'-(3-(4-bromophenyl)-1H-pyrazol-5-yl)-thiourea (IIIa). Prasad et al. reported novel 4, 5-dihydropyrazole derivatives (IV–VI) exhibiting excellent anticancer activity compared to the reference drug cisplatin. Compound having 4-chloro substitution showed excellent anticancer activity (IC_{50} = 4.94 mM) against HeLa (human cervix carcinoma cell lines), which implied that lipophilic and electron-withdrawing halobenzyl groups are beneficial for cytotoxic activity against HeLa cell lines. [12]. Synthesis and anti-cancer activity of a new series of pyrazole chalcones (VIIa–VIIe) against MCF-7 and HeLa cell lines was reported by Sankappa Rai U. et al. Compound VIIc showed the highest inhibition in human MCF-7 and HeLa cell lines; its highest activity was attributed to the 4-fluoro-phenyl and 5-fluoro-pyridin moieties [13].

A series of novel dihydro-pyrano-pyrazole and pyrazolo-pyrimidine derivatives were synthesized and evaluated for their in vitro anticancer activity against the HEPG2 human cancer cell line, and compared to erlotinib and sorafenib as reference drugs. Seven compounds showed nearly 10 fold more activity than erlotinib (10.6μM), with IC_{50} ranging from 0.31 to 0.71μM. In vitro EGFR and VEGFR-2 inhibitory activity were performed for the synthesized compounds, and the results identified compounds to be potent EGFR / VEGFR-2 inhibitors Moreover, two of the compounds revealed potent dual EGFR and VEGFR-2 inhibition. Docking studies showed that compounds interacted with the key amino acids responsible for activity in both enzymes [14].

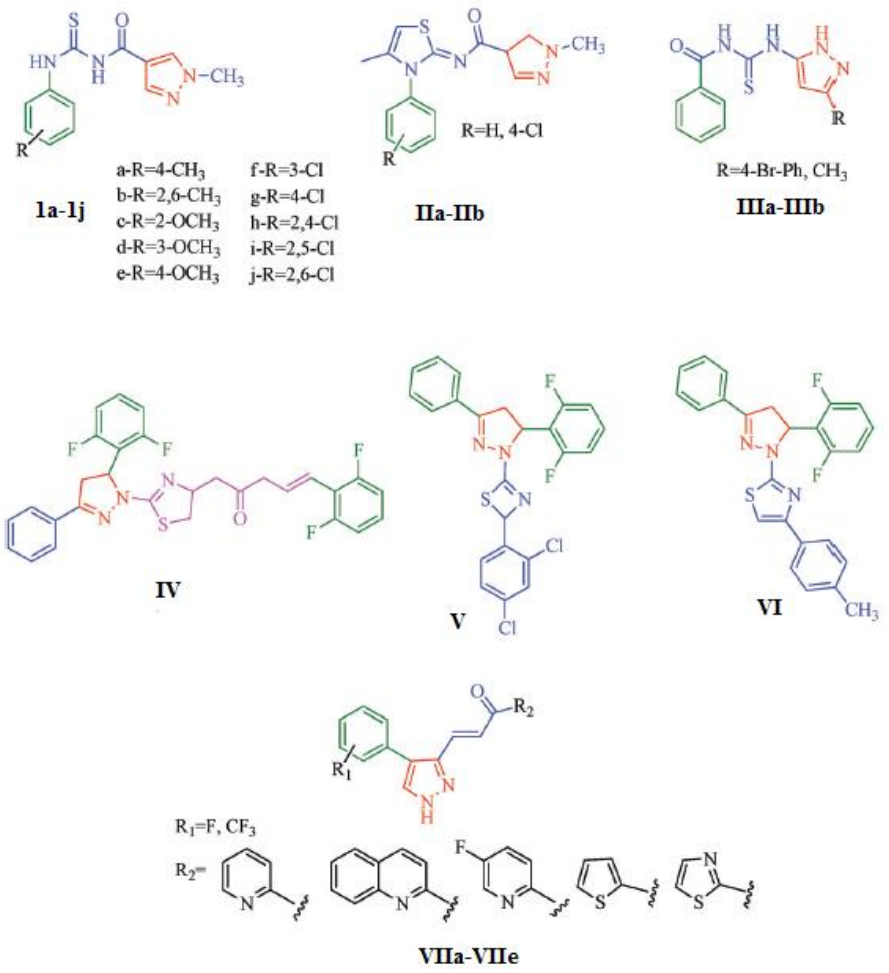

Fig. 2. 1: *Pyrazole derivatives as anticancer agents*

An extensive review by Khalid Karrouchi et al. highlights the different synthesis methods and the pharmacological properties of pyrazole derivatives developed by many researchers around the globe [15].

Thiosemicarbazones (TSCs) are versatile compounds and are well known for their broad pharmacological properties including anticancer activity. Due to their ability to diffuse through the semipermeable membrane of the cell lines, heterocyclic thiosemicarbazones have gained considerable interest in medicinal chemistry. They have been found to show biological activities including anti-tubercular, antibacterial, antimalarial, anti-leprosy, anti-parasitic, antineoplastic, antiviral, antiproliferative, antioxidant and antitumor activities [16].

These compounds are strong inhibitors of ribonucletide reductase, the iron containing enzyme catalyzing the transformation of ribonucleotides to 2'deoxyribonucleotides and hence essential for DNA synthesis and repair [17]. 2-formylpyridine thiosemicarbazone, the first

discovered representative of this class of compounds exhibited potent anticancer activity. Triapine (3-aminopyridine-2-carboxaldehyde thiosemicarbazone) is a well-known representative of this family and was extensively investigated in numerous clinical phase I and II trials in mono or combination therapies. Ribonucleotide reductases are the primary cellular target of Triapine. Two new promising TSCs, namely N′- (6,7-dihydroquinolin-8(5H)-ylidene)-4-(pyridin-2-yl)piperazine-1-carbothiohydrazide (COTI-2, an orally available third generation TSC) and di-2-pyridylketone-4-cyclohexyl-4-methyl-3-thiosemicarbazone (DpC) also entered human clinical studies in the last years, renewing interest in this class of therapeutically-useful compounds [18].

Based on the various bioactivities of these compounds, we have focused on the synthesis of pyrazole thiosemicarbazones derivatives. Here a series of four diphenyl pyrazol thiosemicarbazones (**L1-4**) have been synthesized via general Schiff-base condensation reaction and well characterized by elemental analysis, NMR, FTIR, UV-Vis spectroscopy and mass spectrometry methods.

2.2.2 Materials and instrumentation:

All the chemicals and solvents used for the synthesis and characterization of ligands are of analytical grade and were used as purchased. 1, 3-Diphenyl-1H-pyrazole-4-carboxaldehyde was purchased from Sigma Aldrich; Thiosemicarbazide was purchased from SRL (Sisco research laboratory, Mumbai, India.). ^{1}H NMR spectra were recorded on a Bruker AR X 400 Spectrometer at 400 MHz using DMSO-d^6 as solvent. Mass spectra of the ligands were recorded on Thermoscientific DSQ– II Mass spectrometer. Infrared spectra (400–4000 cm^{-1}) were recorded on α-Bruker FTIR with samples prepared as KBr pellets. C, H and N elemental analysis were performed on a PerkinElmer 240B elemental analyzer. UV spectra were recorded in methanol solution at concentrations around 10^{-3}M on Perkin Elmer Lambda-35 dual beam UV-Vis spectrophotometer.

2.2.3 Synthesis and characterization:

The ligands were synthesized and characterised according to the literature [19]. In brief, an equimolar amount of a substituted thiosemicarbazide (0.01M) and 1, 3-diphenyl-1H-pyrazole-4-carboxaldehyde (0.01 M) was dissolved in 30 ml methanol. The resulting mixture was refluxed for 10 hours in the presence of catalytic amount of glacial acetic acid and the

reaction was monitored by TLC. After completion of the reaction, the mixture was poured into crushed ice. The separated product was filtered wash with cold methanol and dried at room temperature. The resulting white solid was filtered off and dried under vacuum. The ligands were recrystallized in methanol and pure white crystalline product was obtained.

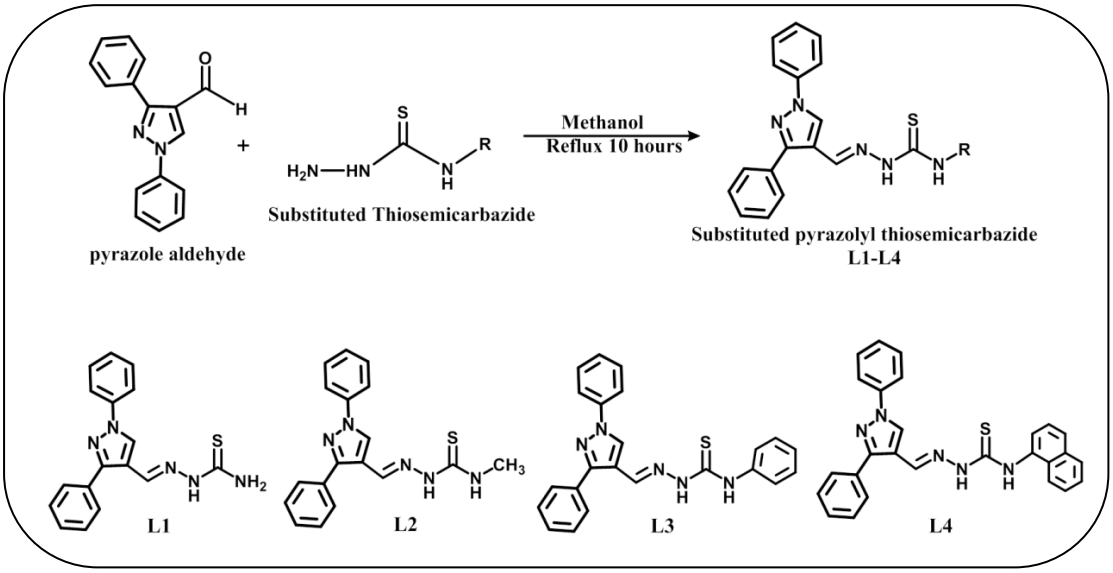

Fig 2.2: *General synthetic route to 1-substituted pyrazolyl thiosemicarbazone* ***L1-4***

1-((1, 3-diphenyl-1H-pyrazol-4-yl)methylene)thiosemicarbazone ***(L1)***

L1 was synthesized by condensation reaction of thiosemicarbazide (2 mmol, 183 mg) and 1, 3-Diphenyl-1H-pyrazole-4-carboxaldehyde (2 mmol, 498 mg). Solubility: MeOH, DMSO, DMF; Yield 79.6 %; Molecular Weight 321.4 g/mol; Molecular Formula $C_{17}H_{15}N_5S$; Colour: White; Anal. Found: C, 63.27; H, 4.32; N, 21.39. Calc.: C, 63.53; H, 4.70; N,21.79 ; MS (m/z) Obs (Calc): 322.2 (321.4) (M^+ + 1); ^{1}H-NMR (DMSO-d^6): δppm 7.37, (tri, 1H, Ar-H); 7.42-7.51, (m,5H, Ar-H); 7.77, (d, 2H, *J* = 6.8 Hz, Ar-H); 7.28, (s, 1H, Ar-H); 7.79, (d, 2H, *J*= 7.6 Hz, Ar-H); 8.03,7.79 (s, 2H, NH_2); 8.36 (s, 1H, HC=N); 10.07, (s, 1H, N-NH); IR (KBr, cm^{-1}): ν(Ar)C-H 2883, *ν*(NNH) 3434; *ν*(NH_2) 3356, 3280; *ν*(C=N) 1599; *ν*(N-N) 1053; *ν*(C=S) assym 1291; *ν*(C=S)sym 816.

1-((1, 3-diphenyl-1H-pyrazol-4-yl)methylene)-4-methyl-3-thiosemicarbazone ***(L2)***

Prepared by condensation of 4-methyl-3-thiosemicarbazide (1.9 mmol, 200 mg) and 1, 3-Diphenyl-1H-pyrazole-4-carboxaldehyde (1.9 mmol, 472 mg). Solubility: MeOH, DMSO, DMF; Yield 80.4 %; Molecular Weight 335.4 g/mol; Molecular Formula $C_{18}H_{17}N_5S$; Colour: pale yellow; Anal. Found: C, 64.11; H, 4.72; N, 20.51. Calc.: C, 64.45; H, 5.11; N, 20.88;

MS (m/z) Obs (Calc): 337.1 (335.4) (M^+ + 2); ^{1}H-NMR (DMSO-d^6): δppm 7.47, (tri, 1H, Ar-H); 7.49-7.59, (m,5H, Ar-H); 7.69, (d, 2H, *J* = 6.8 Hz, Ar-H); 8.22, (s, 1H, Ar-H); 7.91, (d, 2H, *J*= 7.6 Hz, Ar-H); 8.28, (s, 1H, NH-CH_3); 3.03, (s, 3H, N-CH_3); 9.08 (s, 1H, HC=N); 11.41 (s, 1H, N-NH); IR (KBr, cm^{-1}): ν(Ar)C-H 2932, *ν*(NN-H) 3389; *ν*(NH-CH_3) 3325; *ν*(C=N) 1598; *ν*(N-N) 1054; *ν*(C=S) assym 1266; *ν*(C=S)sym 823.

1-((1, 3-diphenyl-1H-pyrazol-4-yl)methylene)-4-phenyl-3-thiosemicarbazone ***(L3)***

Condensation of 4-phenyl-3-thiosemicarbazide (2.9 mmol, 500 mg) and 1, 3-Diphenyl-1H-pyrazole-4-carboxaldehyde (2.9 mmol, 742 mg) yielded **L3**. Solubility: MeOH, DMSO, DMF; Yield 81.06%;Molecular Weight 397.5 g/mol; Molecular Formula $C_{23}H_{19}N_5S$; Colour: Whitish yellow; Anal. Found: C, 69.10; H, 4.47; N, 17.39. Calc.: C, 69.50; H, 4.82; N, 17.62; MS (m/z) Obs (Calc): 398.1(397.5) (M^+ + 1); ^{1}H-NMR (DMSO-d^6): δppm 7.38, (tri, 1H, Ar-H); 7.50-7.58, (m,5H, Ar-H); 7.72, (d, 2H, *J* = 6.7 Hz, Ar-H); 8.34, (s, 1H, Ar-H); 7.92, (d, 2H, *J*= 7.4 Hz, Ar-H); 7.21-7.49, (5H, m, N-C_6H_5); 9.86, (s, 1H, NH-C_6H_5); 9.27, (s, 1H, HC=N); 11.77, (s, 1H, N-NH); IR (KBr, cm^{-1}): ν(Ar)C-H 2964; *ν*(NN-H) 3335; *ν*(NH-C_6H_5) 3290; *ν*(C=N) 1597; *ν*(N-N) 1065; *ν*(C=S)assym 1268; *ν*(C=S)sym 824.

1-((1,3-diphenyl-1H-pyrazol-4-yl)methylene)-4-(naphthalen-1-yl)-3-thiosemicarbazone ***(L4)***

The synthesis of **L4** was carried out by condensation of 4-(1-naphthyl)-3-thiosemicarbazide (1.6 mmol, 350 mg) and 1, 3-diphenyl-1H-pyrazole-4-carboxaldehyde (1.6 mmol, 399 mg). Solubility: MeOH, DMSO, DMF; Yield 85.4 %; Molecular Weight 447.2 g/mol; Molecular Formula $C_{27}H_{21}N_5S$; Colour: yellow; Anal. Found: C, 72.22; H, 4.38; N, 15.41. Calc.: C, 72.46; H, 4.73; N, 15.65; MS (m/z) Obs (Calc): 448.1 (447.2) (M^+ + 1); ^{1}H-NMR (DMSO-d^6): δppm 7.34, (tri, 1H, Ar-H); 7.56-7.58, (m,5H, Ar-H); 7.75, (d, 2H, *J* = 6.8 Hz, Ar-H); 7.75, (s, 1H, Ar-H); 7.88, (d, 2H, *J*= 8.6 Hz, Ar-H); 7.46-7.56, (7H, m, N-$C_{10}H_7$); 10.17, (s, 1H, NH- $C_{10}H_7$); 9.26, (s, 1H, HC=N); 11.88, (s, 1H, N-NH); IR (KBr, cm^{-1}): ν(Ar)C-H 2971; *ν*(NN-H) 3334; *ν*(NH-$C_{10}H_7$) 3123; *ν*(C=N) 1597; *ν*(N-N) 1047; *ν*(C=S)assym 1276; *ν*(C=S)sym 807.

2.2.4 Results and discussion:

Electronic spectroscopy is a very important tool for the structural identification of synthesized pyrazolyl thiosemicarbazone derivatives. The UV spectra show bands in the wavelength range 200-700 nm. The first band appearing within 223-227 nm regions can be assigned to the π→π* transition of the aromatic rings (*Fig. 2.3*). The second band observed

within 313-365 nm region is due to the excitation of the electrons of the azomethine group which corresponds to an intra-ligand $n \rightarrow \pi^*$ transition [20]. The peak values have been tabulated in Table 2.1.

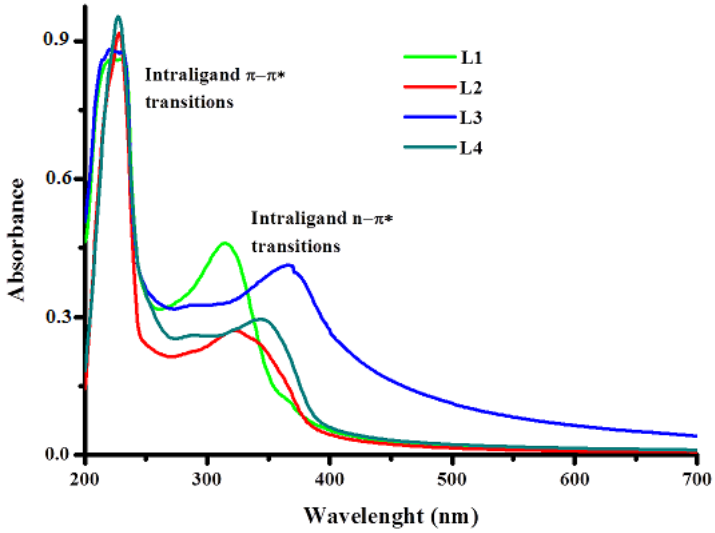

Fig. 2.3: *UV spectra of ligands* ***L1-4*** *recorded in MeOH with path length 1 cm.*

Table 2.1: UV peak assignments of **L1-4**

Code	L1	L2	L3	L4
Intra-ligand transitions(nm) π-π*	223	227	224	227
Intra-ligand transitions(nm) n-π*	313	322	365	346

Mass spectral data confirm the structure of the ligand as indicated by the molecular ion peak corresponding to their molecular weight. The MS spectra of the ligands (*Fig. 2.4*) showed molecular ion peaks 322.2 ($M^+ + 1$) for **L1,** 337.1 ($M^+ + 2$) for **L2,** 398.1 ($M^+ + 1$) for **L3** and 448.1 ($M^+ + 1$) for **L4** which is well in agreement with the proposed composition. The molecular ion peaks have been provided in Table 2.2

Table 2.2: m/z values of Ligands

Code	L1	L2	L3	L4
Calculated Mass (g/mol)	321.4	335.4	397.5	447.2
Observed Mass (g/mol)	322.2 ($M^+ + 1$)	337.1 ($M^+ + 2$)	398.1 ($M^+ + 1$)	448.1 ($M^+ + 1$)

In the IR spectra, of the ligands, significant stretching bands due to -NN-H was observed at 3434 cm^{-1}, 3389 cm^{-1}, 3335 cm^{-1} and 3334 cm^{-1} for **L1**, **L2**, **L3** and **L4** respectively, while stretching bands due -N-N- were observed at 1053cm^{-1} for **L1**, 1054 cm^{-1} for **L2**, 1065 cm^{-1} for **L3** and 1047 cm^{-1} for **L4**. Asymmetric and symmetric -C=S stretching bands are observed in **L1-4** in the range of 1291-1266 cm^{-1} and 807-824 cm^{-1} respectively. The characteristic -CH=N- bands for the thiosemicarbazone derivatives were observed at 1599 cm^{-1}, 1598 cm^{-1}, 1597cm^{-1} and 1597 cm^{-1} for **L1**, **L2**, **L3** and **L4** respectively . Additional bands for **L1** (ν_{NH-H}) at 3356 cm^{-1} and 3280 cm^{-1}, **L2** (ν_{NH-CH3}) at 3325 cm^{-1}, **L3** ($\nu_{NH-C6H5}$) at 3290 cm^{-1} and **L4** ($\nu_{NH-C10H7}$) at 3123 cm^{-1} were also observed in the spectra of the ligands [21].

In the ^{1}H NMR spectra as shown in *Fig. 2.5*, the signals due to (-C**H**=N-) proton, appeared in these compounds at 8.36 ppm (**L1**), 9.08 ppm (**L2**), 9.27 ppm (**L3**) and 9.26 ppm (**L4**) respectively as singlets, conforming the formation of Schiff bases via condensation reaction between the thiosemicarbazide and 1, 3-diphenyl-1H-pyrazole-4-carboxaldehyde. Apart from this, signals due to the proton of N**H**-R (R =H, CH_3, C_6H_5, $C_{10}H_7$) are observed respectively at 8.03 ppm **,** 8.28 ppm**,** 9.86 ppm and 10.17 ppm for **L1, L2, L3** and **L4** as singlets. The imine N-N**H** protons appeared as sharp singlets at the most downfield region in the NMR spectra of all the ligands (**L1** 10.07 ppm, **L2** 11.41 ppm, **L3** 11.77 ppm and **L4** 11.88 ppm). Rest all the aromatic protons due to pyrazole moiety as well as substituted phenyl group were observed in the expected regions as discussed in section 2.2.3. It was clearly observed from ^{1}H NMR spectra that the signals corresponding to the N**H**-R protons shifted downfield as the substituting group (R) was changed. This might suggest that the R is affecting the electronic nature of the thioamide bond. The δ value shifted 8.28 to 10.17 ppm in a following sequences H **(L1)** < CH_3 **(L2)** < C_6H_5 **(L3)** < $C_{10}H_7$ **(L4)** mainly this shift is due to the electron density redistribution of proton present in cone of phenyl ring in **L3** and **L4**.

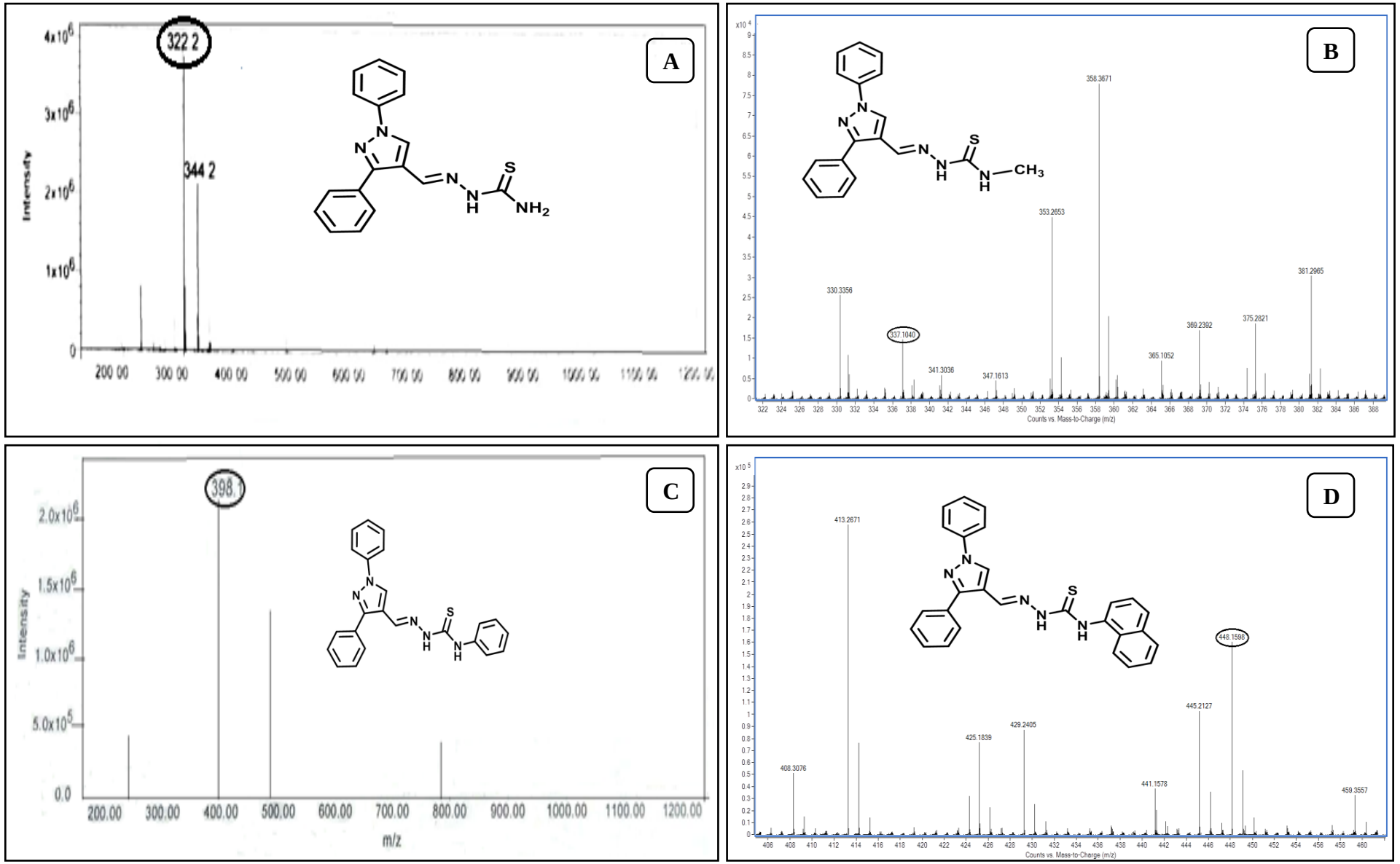

Fig. 2.4: *ESI-MS spectra of ligands (A)* ***L1*** *(B)* ***L2*** *(C)* ***L3*** *(D)* ***L4*** *indicating their molecular ion peak*

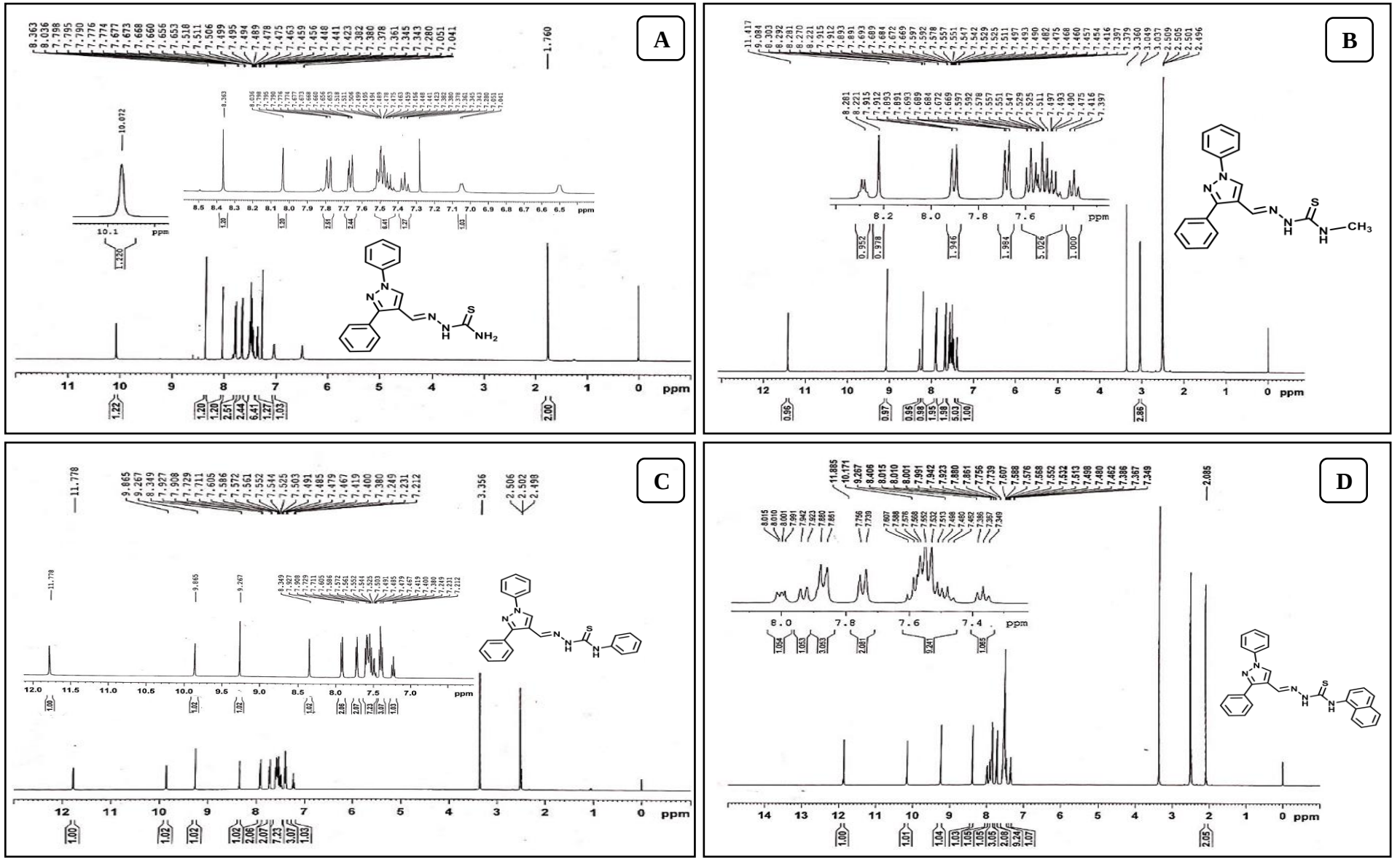

Fig. 2.5: *^{1}H NMR spectra of ligands (A)* ***L1*** *(B)* ***L2*** *(C)* ***L3*** *(D)* ***L4***

2.3 Diphenylpyrazol α-Amino acid derivatives (L5-L8):

2.3.1 Introduction:

Designing of new molecules as anticancer agents, require simulation of a suitable bioactive pharmacophore. The pharmacophore should not only be potent but must also be safe on normal cell. Amino acids are by far the most important low-molecular-weight ligands in biological systems. The therapeutic use of amino acids presents a viable and important option for natural medicine. Moreover, natural-occurring amino acids are interesting moieties in organic synthesis with several advantages, such as easy access, low cost, presence of one or more defined stereocenters and the possibility of functionalization in both the amine or carboxyl end. Furthermore, an increased amino acid uptake has been described for some types of cancer, making it a promising building block for enhancing the selectivity towards cancer cells. Finally, some anticancer drugs, such as Melphalan and Eflornithine, have a substituted amino acid scaffold whereas both of the well-known anticancer drugs, Paclitaxel and Docetaxel have amino acids side chain.

A series of functionalized amino acid derivatives 1-N-substituted-3-amino-2-hydroxy-3-phenylpropane-1-carboxamide and N-substituted 1-N-(tert-butoxycarbonyl)-2,2-dimethyl-4-phenyl-5- oxazolidine carboxamide were synthesized and evaluated for their in vitro cytotoxicity against human cancer cell lines. Some of the compounds showed promising cytotoxicity in ovarian and oral cancers [22].

The amino acid derivatives of 5, 11-dimethyl-5H-indolo[2,3-b]quinoline (DiMIQ) were synthesized by the reaction of its 9-aminoderivative with selected amino acids such as glycine, L-proline, D-proline, L-histidine, and D-histidine . The peptide derivatives of DiMIQ were also synthesized. Most of the compounds exhibited a high *in vitro* antiproliferative activity and effectively inhibited growth of tumor in mice compared to the parent compound. The conjugation of the hydrophilic amino acid / peptide to the hydrophobic DiMIQ increased its hydrophilicity and decreased its hemolytic activity. The glycylglycine conjugate was the most promising derivative. It strongly inhibited the growth of the tumor in mice and significantly lowered the *in vivo* toxicity compared to DiMIQ [23].

Glutamic acid and its derivative glutamine are known to play interesting roles in cancer genesis, hence, it was realized that structurally different glutamic acid derivatives may be

designed and developed, with antagonistic effects on cancer. An article by Imran Ali et al. describes the state-of-art of glutamic acid and its derivatives as anticancer agents. Moreover the mechanism of action of glutamic acid derivatives as anticancer agents, clinical applications of glutamic acid derivatives, as well as recent developments and future perspectives of glutamic acid drug development have also been discussed [24].

Acridinyl amino acid derivatives have been found to display good antitumor activity. Gellerman described the synthesis of N-substituted 9-aminoacridine and bis-acridine derivatives containing electron-withdrawing or electron-donating groups, including amino acid residues. These derivatives showed higher antitumor activity in comparison with parent 9-aminoacridine, probably due to enhancement of biologically important chelating properties leading to formation of more strong DNA damaging reactive species. Singh and co-workers reported the synthesis of acridone - amino acid derivatives as potential leads to anticancer drugs, while Gao and co-workers developed amino acid acridone analogues possessing a 3, 5-dimethoxyphenyl moiety. According to the studies, cell death can be caused by multiple mechanisms, such as inhibition of aerobic glycolysis, mitochondrial oxidative phosphorylation, DNA damage and oxidative stress. Lyakhov et al. synthesized a series of 9-acridine amino acid derivatives and showed that the antiproliferative activity of these compounds depends on the selected amino acid and its chain length [25].

A series of dual-protected amino acid derivatives was synthesized and evaluated as potential novel anticancer agents. The cytotoxic activities were screened *in vitro* against a panel of tumor and non-tumor cells using 3-(4,5-dimethylthiazol-2-yl)-2,5-diphenyltetrazolium bromide (MTT) assay. Among the synthesized derivatives, three of them showed promising activity against cancer cells with half-maximal inhibitory concentration (IC_{50}) ranging between 1.7-6.1 μM. The most promising derivative, bearing both a lipophilic *N*-alkyl diamine moiety and a protected amino acid scaffold showed a selectivity index of 3.4 towards tumor cells. The *N*-alkyl diamine moiety seems to play a crucial role in the enhancement of the anticancer activity. On the other hand, the incorporation of an amino acid scaffold resulted in increase in the selectivity towards cancer cell lines [26].

Apart from the therapeutic use of amino acid derivatives, the aryl pyrazole derivatives are also well known for their antiproliferative properties against several kinds of human tumor cell lines as previously mentioned (section 2.2.1). Keeping this perspective in mind, herein

we report the synthesis of four new N-[(1, 3-diphenylpyrazol-4-yl) methyl] α-amino acids with the aim to have promising biological activity.

2.3.2 Materials and instrumentation:

1, 3-Diphenyl-1H-pyrazole-4-carbaldehyde was purchased from Sigma Aldrich as mentioned previously. The α-Amino acids were purchased from SRL (Sisco research laboratory, Mumbai, India.). All the four ligands were characterized by elemental analysis and various spectral techniques (ESI-MS, IR, UV-Vis and ^{1}H-NMR). Detailed instrumentation is given in section 2.2.2.

2.3.3 Synthesis and characterization:

The ligands were synthesized according to the literature [27]. Amino acid (2.76 mmol) and NaOH (2.76 mmol) in dry methanol (5 ml) were stirred for 30 min to get a homogeneous solution. A methanolic solution (5 ml) of 1,3-Diphenyl-1H-pyrazole-4-carboxaldehyde (2.76 mmol) was added dropwise to the above solution, which was refluxed for 90 min, cooled, and treated with $NaBH_4$ (5.2 mmol) with constant stirring for 2 h. The solvent was evaporated, the resulting mass was dissolved in water and acidified with dilute HCl, and the solution pH was maintained within 5–6. The ligand that precipitated out was filtered, thoroughly washed with water and then with cold methanol. The compounds were recrystallized from hot methanol and finally dried in vacuum. Yields were in the range of 70-80% and the ligands were soluble in MeOH, DMSO and DMF.

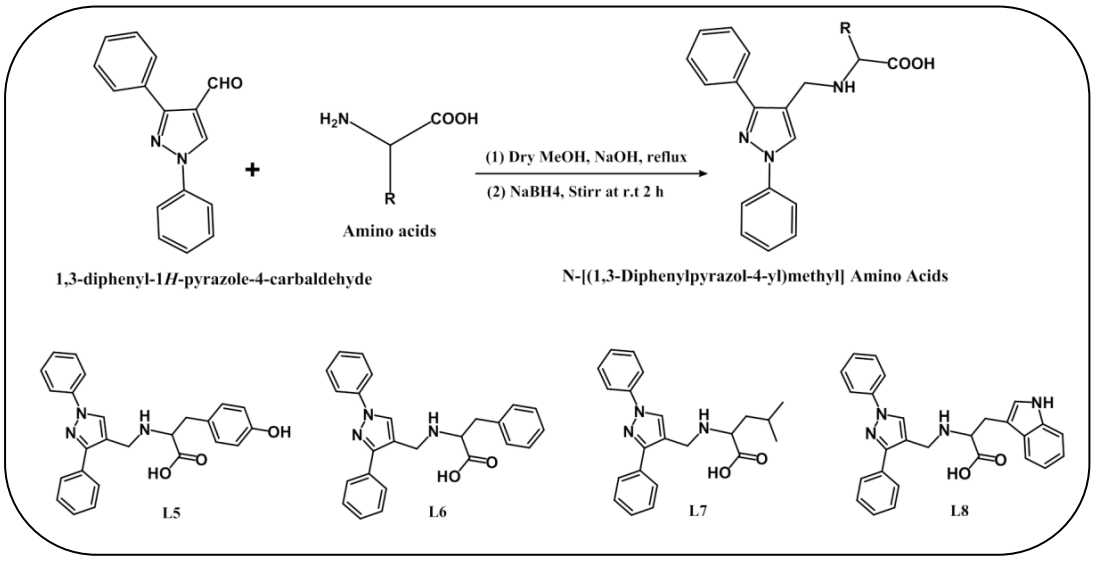

Fig 2.6** General synthetic route to N-[(1,3-diphenylpyrazol-4-yl)methyl] α-amino acids **L5-8

((1,3-diphenyl-1H-pyrazol-4-yl)methyl)tyrosine ***(L5)***

L5 was prepared by condensation of tyrosine (1.0 mmol, 190 mg) and 1, 3-Diphenyl-1H-pyrazole-4-carboxaldehyde (1.0 mmol, 260 mg) followed by $NaBH_4$ reduction. Yield 79.23 %; Molecular Weight 413.5 g/mol; Molecular Formula $C_{25}H_{23}N_3O_3$; Colour: White; Anal. Found: C, 72.68; H, 5.71; N, 10.17. Calc.: C, 72.62; H, 5.61; N, 10.16; MS (m/z) Obs (Calc): 414.6 (413.5) (M^+ + 1); ^{1}H-NMR (DMSO-d^6): δppm 9.32 (s, 1H, -OH of tyrosine),7.48-7.37 (m, 4H, Ar-H of tyrosine); 7.04, (tri, 1H, Ar-H); 7.74-7.52, (m,5H, Ar-H); 7.77, (d, 2H, *J* = 4.8 Hz, Ar-H); 8.25, (s, 1H, Ar-H); 7.81, (d, 2H, *J*= 7.6 Hz, Ar-H); 3.87, (s,1H, N-H); 2.87, (s, 2H, CH_2-Ph); IR (KBr, cm^{-1}): νO-H 3423, νN-H 3139, νC=O 1601; *ν*(Ar–C-H) 2860.

((1,3-diphenyl-1H-pyrazol-4-yl)methyl)phenylalanine ***(L6)***

Prepared by condensation of phenylalanine (1.1 mmol, 185 mg) and 1, 3-Diphenyl-1H-pyrazole-4-carboxaldehyde (1.1 mmol, 277 mg) followed by reduction with $NaBH_4$. Yield 72.15 %; Molecular Weight 397.5 g/mol; Molecular Formula $C_{25}H_{23}N_3O_2$; Colour: White; Anal. Found: C, 75.56; H, 5.89; N, 10.63. Calc.: C, 75.55; H, 5.83 ; N, 10.57 ; MS (m/z) Obs (Calc): 398.6 (397.5) (M^++1); ^{1}H-NMR (DMSO-d^6): δppm 7.25-7.27 (m 5H, Ar-H of phenylalanine),7.37, (tri, 1H, Ar-H); 7.51, (m,5H, Ar-H); 7.67, (d, 2H, *J* = 6.8 Hz, Ar-H); 8.32, (s, 1H, Ar-H); 7.82, (d, 2H, *J*= 7.6 Hz, Ar-H); 3.90, (s,1H, N-H); 3.52, (s,2H, CH_2-Ph); IR (KBr, cm^{-1}): νO-H 3510, νN-H 3272, νC=O 1598; *ν*(Ar–C-H) 2818.

((1,3-diphenyl-1H-pyrazol-4-yl)methyl)leucine ***(L7)***

Condensation of leucine (1.5 mmol, 200 mg) and 1, 3-Diphenyl-1H-pyrazole-4-carboxaldehyde (1.5 mmol, 378 mg) followed by reduction yielded the desired product. Yield 85.13 %; Molecular Weight 363.5 g/mol; Molecular Formula $C_{22}H_{25}N_3O_2$; Colour: Whitish yellow; Anal. Found: C, 72.64; H,7.10 ; N, 11.70 Calc.: C, 72.70; H, 6.93; N, 11.56; MS (m/z) Obs (Calc): 364.6 (363.5) (M^++1); ^{1}H-NMR (DMSO-d^6): δppm 0.82-1.85 (d, 6H, leucine-iso-prop-$(CH_3)_2$); 7.38, (tri, 1H, Ar-H); 7.43-7.53, (m,5H, Ar-H); 7.85, (d, 2H, *J* = 5.8 Hz, Ar-H); 8.53, (s, 1H, Ar-H); 7.88, (d, 2H, *J*= 7.6 Hz, Ar-H); 4.55, (s,1H, N-H); 3.65, (t,2H, CH_2-iso propyl); IR (KBr, cm^{-1}): νO-H 3446, νN-H 3058, νC=O 1616; *ν*(Ar–C-H) 2957.

((1,3-diphenyl-1H-pyrazol-4-yl)methyl)tryptophan ***(L8)***

Reaction of tryptophan (1.1 mmol, 240 mg) and 1, 3-Diphenyl-1H-pyrazole-4-carboxaldehyde (1.1 mmol, 291 mg) followed by reduction gave the product. Yield 82.98 %; Molecular Weight 436.5 g/mol; Molecular Formula $C_{27}H_{24}N_4O_2$; Colour: White; Anal. Found: C, 74.36; H, 5.63; N, 13.03. Calc.: C, 74.29 ; H, 5.54 ; N, 12.84; MS (m/z) Obs (Calc): 437.6 (436.5) (M^++1); ^{1}H-NMR (DMSO-d^6): δppm 10.87 (s, 1H, Indolinic N-H of tryptophan); 7.04, (tri, 1H, Ar-H); 7.45-7.56, (m,5H, Ar-H); 7.73, (d, 2H, *J* = 6.8 Hz, Ar-H); 8.27, (s, 1H, Ar-H); 7.90, (d, 2H, *J*= 8.6 Hz, Ar-H); 4.55, (s,1H, N-H); 3.13, (s,2H, CH_2-Indole); IR (KBr, cm^{-1}): νO-H 3457, νN-H 3344, νC=O 1595; *ν*(Ar–C-H) 2824.

2.3.4 Results and discussion

The four Diphenylpyrazol α-Amino acid derivatives have been synthesized according to the general synthetic route given in *Fig. 2.6* in good yields.

The composition and structures of all the four Diphenylpyrazol α-Amino acid derivatives have been confirmed by ^{1}H NMR, Mass spectrometry, infrared spectroscopy and UV spectroscopy. The analytical data are consistent with the proposed structures and their empirical formulae. The UV spectra of the ligands **L5-8** in methanol (*Fig. 2.7*) was carried out in the region 200-400 nm. Two major bands were observed in this region, first peak ascribed to π→π* intra ligand transition around 227-230 nm and second band observed with medium intensity ascribed to *n*→π* intra ligand transition in the region 270-272 nm because of the presence of chromophoric group in pyrazole as well as amino acid moiety present in diphenylpyrazol α-amino acid derivatives. The peak values have been tabulated in Table 2.3.

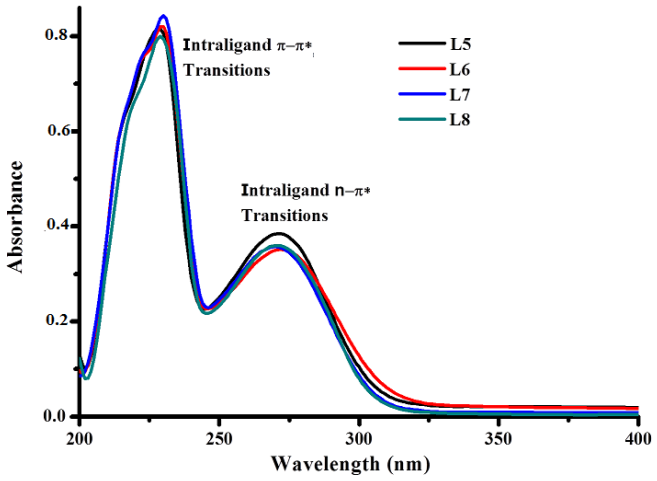

Fig. 2.7: *UV spectra of ligands* ***L5-8*** *recorded in MeOH with path length 1 cm*

Fig. 2.8 shows the fluorescence spectra of the diphenylpyrazol α-amino acid derivatives recorded in methanol. Ligands **L6** and **L7** exhibited strong fluorescence emission at 344 and 345 nm whereas **L5** and **L8** showed less intense fluorescene at 343 and 347 nm respectively (Table 2.3) when excited at 269 nm .

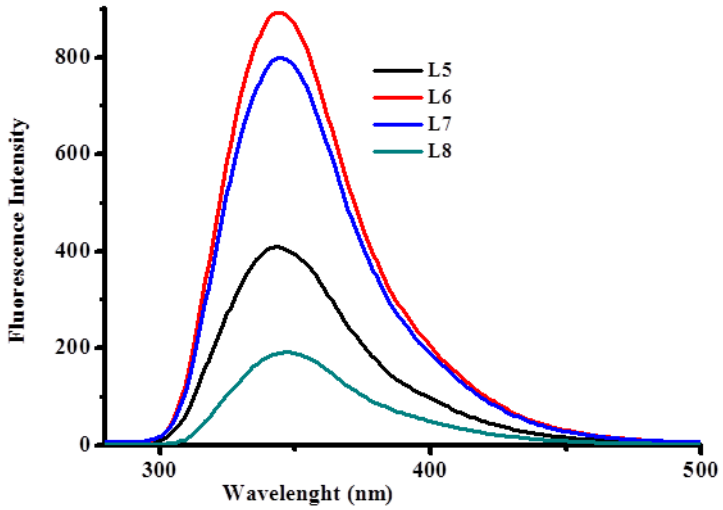

Fig 2.8: *Fluorescence spectra of complexes **L5-8** recorded in MeOH with path length 1cm.*

Table 2.3: UV peak and emission peak assignments of **L5-8**

Code	L5	L6	L7	L8
Intra-ligand transitions(nm) π-π*	228	229	230	229
Intra-ligand transitions(nm) n-π*	271	271	272	270
$\lambda_{em.}$ ***(nm)***	343	344	345	347

The ESI-MS spectra of the ligands **L5-8** (*Fig. 2.9*) showed molecular ion peaks corresponding to M^+ +1 species at 414.6, 398.6, 364.6 and 437.6 for **L5, L6, L7** and **L8** respectively which are in well agreement with the proposed composition. The m/z peaks are tabulated in Table 2.4.

Table 2.4: m/z values of Ligands

Code	L5	L6	L7	L8
Calculated Mass (g/mol)	413.2	397.5	363.5	436.2
Observed Mass (g/mol)	414.6 (M^++1)	398.6 (M^++1)	364.6 (M^++1)	437.6 (M^++1)

Selected diagnostic bands in the IR spectra of the synthesized Diphenylpyrazol α-Amino acid derivatives revealed useful information about the structure of the compounds. The IR spectra displayed strong C=O stretching bands for **L5, L6, L7** and **L8** at 1601 cm^{-1}, 1598 cm^{-1}, 1616 cm^{-1} and 1595 cm^{-1} respectively due to the carboxylic acid group of the amino acids. A distinct broad band at 3423 cm^{-1} (**L5**), 3510 cm^{-1} (**L6**), 3446 cm^{-1} (**L7**) and 3457 cm^{-1} (**L8**) owing to the O-H stretching of free carboxylic acid group was observed for all the ligands. The characteristic medium intensity secondary amine N-H stretching bands were observed at 3139 cm^{-1}, 3272 cm^{-1}, 3058 cm^{-1} and 3344 cm^{-1} for **L5**, **L6**, **L7** and **L8** respectively.

The ^{1}H NMR spectra of ligands **L5-8** (*Fig. 2.10*) the major signals were due secondary imine N-**H** proton of the mannich bases at 3.87 ppm (**L5**), 3.90 ppm (**L6**) 4.55 ppm (**L7**) and 4.55 ppm (**L8**). The spectrum of **L5** (*Fig. 2.10*, A) show 1 proton broad singlet at δ = 9.32 ppm owing to –O**H** of tyrosine and 4 multiplet aromatic proton of tyrosine at δ = 7.48 – 7.37 ppm in a downfield region. In the spectrum of **L6** (*Fig. 2.10*, B) the 5 aromatic proton showing multiplet at 7.25-7.27 ppm is because of phenylalanine moiety. A 6 proton singlet at δ = 0.82-1.85 ppm owing to two methyl groups –CH $(CH_3)_2$ of leucine is observed in the spectrum of **L7** (*Fig. 2.10*, C). The spectrum of **L8** (*Fig. 2.10*, D) shows a 4 proton multiplet in the δ range of 6.95-7.56 ppm ascribable to the aromatic protons of the tryptophan and a 1 proton singlet at δ = 10.87 ppm attributed to the indoyl N-**H**. Rest all aromatic protons were attributed to diphenyl pyrazole ring within the range 7.04 – 8.53 ppm as mention above in section 2.3.3.

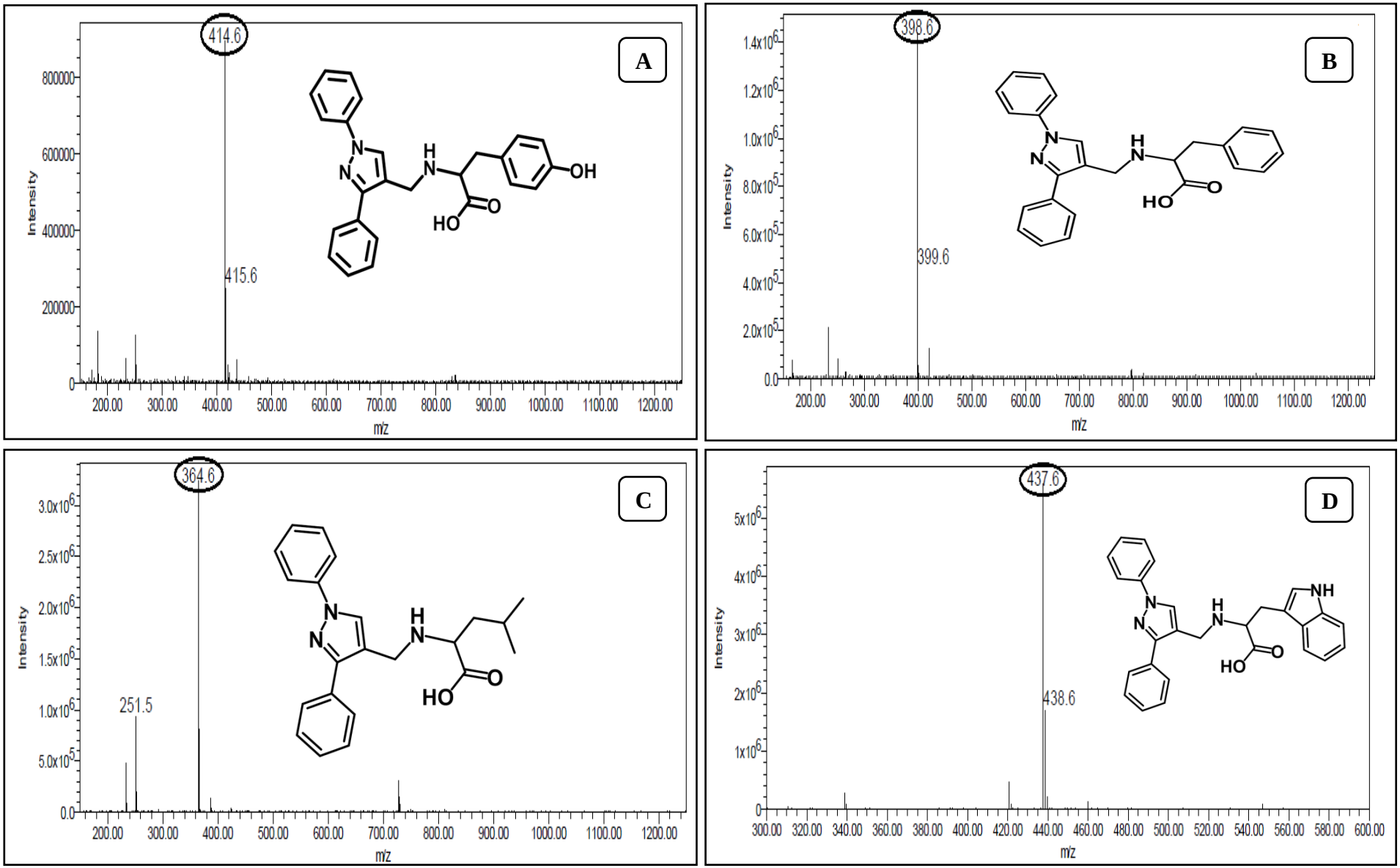

Fig. 2.9: *ESI-MS spectra of ligands (A)* ***L5*** *(B)* ***L6*** *(C)* ***L7*** *(D)* ***L8*** *indicating their molecular ion peak*

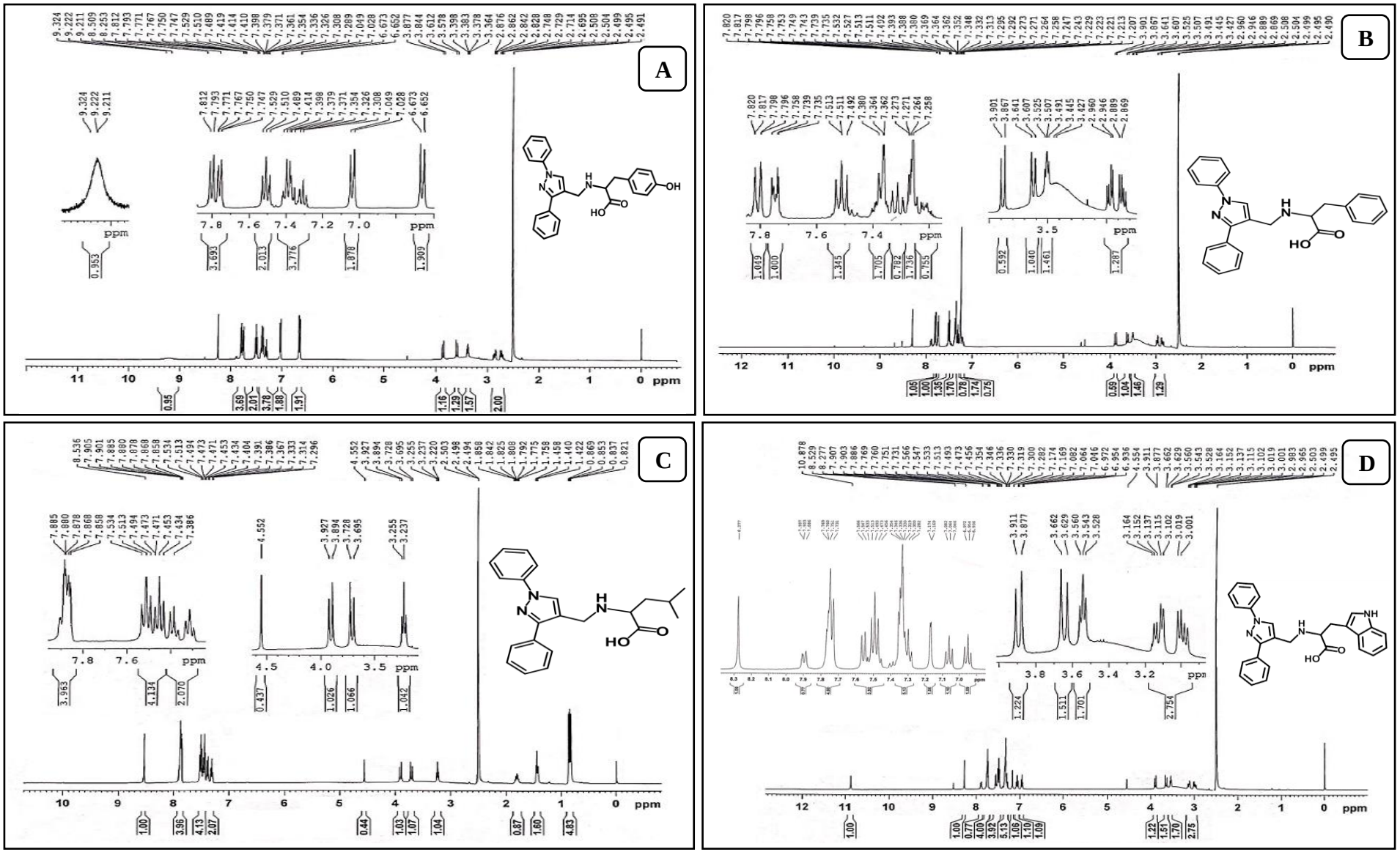

Fig. 2.10: *^{1}H NMR spectra of ligands (A)* ***L5*** *(B)* ***L6*** *(C)* ***L7*** *(D)* ***L8***

2.4 Ferrocenyl thiosemicarbazones (L9-L12):

2.4.1 Introduction:

Ferrocene derivatives have been reported to exhibit antiproliferative activity against several cancer cell lines with low toxic effects when compared to known anticancer agents. Ferrocene displays distinct redox behaviour whereby it oxidizes readily to ferricenium ion (Fc^+), an unusually stable radical cation. Its electron transfer and free radical reactions are useful in biological processes. Some of the important biological reactions of ferrocene analogues are reduction of Fc^+ by NADH and metalloproteins; oxidation of ferrocene by hydrogen peroxide catalyzed by enzymes; recombination of the ferricenium system with an attack on free radicals leading to substituted ferrocene upon proton elimination. Fc^+ reacts with biologically important superoxide anion radicals, resulting in the regeneration of ferrocene and dioxygen. In cancer cytology, free-radical chemistry plays a vital role in the different phases of growth and control of tumour [28].

The superoxide and the free radical-scavenging reaction of ferrocene are useful in the inhibition of cancer growth. Furthermore, the reaction of Fc^+ with the free-radical form of ribonucleotide reductase, an important enzyme for DNA synthesis, makes ferrocene a useful scaffold for the development of potent anti-cancer compounds [28]. The aforementioned factors have prompted research on the development of ferrocene derivatives with enhanced biological activity. An extensive review by S. Peter and B.A. Aderibigbe describes the syntheses and anti-cancer activities of various ferrocene conjugated compounds some of which have been discussed in brief [29].

Ferrocene–Indole Hybrids

Indoles are cheap and have unique anticancer properties. Combining ferrocene and indole derivatives into hybrid compounds is a potential route for the development of effective anticancer drugs. Quirante et al. synthesized and evaluated the ferrocenyl–indole derivatives with ferrocene moiety attached on C-3 of the 2-phenylindole skeleton for anticancer activity using an A549 human lung carcinoma cell line. Some of the compounds exhibited potent cytotoxic effect against the cancer cell lines with IC_{50} values in the range of 5- 10 μM. All the ferrocenyl–indole derivatives were more active when compared to their parent drugs. The nature of the substituents on C-5 of the indole ring and halogen substituents on the para

position of aryl ring played a significant role on the cytotoxic effect of the hybrid molecules [30].

1,2,4-Trioxane–Ferrocene Hybrids

1,2,4-trioxane ferrocene derivatives were reported by Reiter et al. as potential drugs for various biological activities such as antimalarial, anticancer. The molecular weight and number of 1,2,4-trioxane moieties present in these compounds played an important role in their cytotoxic effects against CEM/ADR5000 cell in vitro. Compound with two moieties and a molecular weight of 800 g/mol exhibited enhanced cytotoxic effects when compared to compound with one moiety and a molecular weight of 500 g/mol [31].

Ferrociphenols

Ferrociphenols are reported as the most active antiproliferative agents when compared to cisplatin and tamoxifen cancer drugs. They have diverse modes of action which are caused by the redox behaviour of the ferrocenyl moiety, in the cancer cell [32]. Their target is the mitochondrial system or redox proteins in the cancer cells [33]. The position of the oxidizable ferrocenyl group was reported to play a major role in the antiproliferative activity of the compounds [34]. Plazuk et al. reported the synthesis of ferrocenyl compounds with ferrociphenols and a 1H-1,2,3-triazolyl moiety acting as a linker and their cytotoxic activities against human breast cancer cells (HCC38 and MCF-7) in vitro. Some of the compounds exhibited good cytotoxic activity against the hormone-independent HCC38 breast cancer cell line. The most active compound was with IC_{50} = 15.3 μM and it contained a para hydroxyphenyl group. The introduction of two para-hydroxyphenyl moiety resulted in a decrease in the anticancer activity of the compound with an IC_{50} value of 30.6 μM. The introduction of a 3,5-dihydroxyphenyl led to a significant decrease in the anticancer activity [35].

Ferrocenyl Derivatives of Clotrimazole Drug

Pedotti et al. reported the synthesis of two ferrocenyl–clotrimazole derivatives by replacing one of the phenyl rings in the clotrimazole structure with a ferrocene moiety and studied their growth inhibition effects against two human cancer cell lines, colorectal cancer cells HT29 and breast cancer cells MCF-7.The ferrocenyl–clotrimazole derivatives were more active against breast cancer cell MCF-7 when compared to the colorectal cancer cell line HT29. These two compounds were more active than their parent drug clotrimazole. The

modification of the structure with ferrocene enhanced the cytotoxic activity of the compounds when compared to the parent drug. The aforementioned enhanced effect is attributed to the redox properties of iron in the ferrocene moiety and also its ability to generate cytotoxic reactive oxygen species [36].

Ferrocenyl Chalcogeno Triazole Conjugates

Panaka et al. reported the synthesis of ferrocenyl–chalcogeno derivatives and evaluated their cytotoxic activity against five different cancer cell lines (A549, MDA-MB-231, MCF-7, HeLa, and HEK-239T). The IC_{50} values of the compounds ranged between 2.9 and 20 μM for the first four cancer cells, and none of the compounds were effective against HEK-239T. The derivatives with selenium exhibited higher cytotoxicity with IC_{50} values ranging between 2.9 and 18.3 μM compared to the sulfur derivatives with inhibition values between 4.46–18.9 μM, respectively [37]. The higher activity of the compounds with Se is attributed to its antioxidant property, ability to modulate carcinogen metabolism and inhibit tumor cell growth.

Ferrocenyl–Olefin Derivatives

Oliveira et al. studied the antiproliferative effect of tetrasubstituted olefins–ferrocenyl compounds on different human cancer cells such as MDA-MB-435(human melanoma), SF-295 (human glioblastoma), HCT-8 (human colon cancer), and HL-60 (human promyelocytic leukemia). An MDA-MB-435 cell line was found to be highly sensitive to the compounds with amine side chains which contributed to estrogen–receptor interactions. The introduction of an aromatic substituent did not play an important role in the cytotoxicity activity of the compounds against MDA-MB-231 cells. A less bulky substituent such as acetyl enhanced the cytotoxic effect compared to a pivaloyl substituent against the selected cancer cell lines [38]. Jadhav et al. synthesized a series of ferrocenyl chalcone and amidines and the compounds were tested in vitro for anticancer activity against human breast cancer cell line MDA-MB-435. Some of these compounds exhibited good anticancer activity when compared to doxorubicin against MDA-MB-435 cancer cell lines with GI_{50} values between 16.85–63.2 μM [39].

Ferrocene–Carboxylate Derivatives

Perez et al. synthesized ferrocene derivatives containing carboxylate and acetylate and investigated their antiproliferative activity in vitro against MCF-7, MCF-10A, and HT-29

cancer cell lines using an MTT assay. The compounds exhibited moderate to low antiproliferative activity with IC_{50} values in the range of 45.5 – 103 μM against MCF-7 breast cancer cell lines but did not exhibit any significant activity against HT-29 and MCF-10A with inhibition values between 121–298 μM [40].

Vera et al. reported the synthesis and evaluated the antiproliferative activity of ferrocene–carboxylate compounds with phenyl and halogen (F, I, Cl, and Br). The compounds exhibited high activity against MCF-7 and MCF-10A cancer cells. The in vitro anti-proliferative studies also indicated that the compounds with 4-fluorophenyl substituent have no cytotoxic effect on the cancer cell lines [41].

Ferrocene Incorporated Selenourea Derivatives

Hussain et al. synthesized ferrocene incorporated with selenourea derivatives and tested them for their in vitro anticancer activity against liver cancer (Hepa 1c1c7), breast cancer (MCF-7), and neuroblastoma (MYCN2 and SK-N-SH). Only four compounds exhibited moderate anticancer activity against the aforementioned cells. The cytotoxic effects of the compounds were significantly influenced by the ortho substitution on the phenyl ring attached with the carbonyl carbon [42].

Ferrocene–Steroid Conjugates

Pita et al. reported the synthesis of ferrocene–steroid conjugates and evaluated their anticancer activity against colon cancer HT-29 and breast cancer MCF-7 cell lines. The compounds exhibited good antiproliferative activity with IC_{50} values less than 30 μM against the MCF-7 breast cancer cell line when compared to tamoxifen with an IC_{50} of 47 μM at low concentration. One of the compounds showed high antiproliferative activity with an inhibition value of 1.2 μM, exceeding that of cisplatin against the HT-29 colon cancer cell line [43]. The presence of ferrocene moiety in the compounds enhanced the anti-proliferative activity against the HT-29 colon cancer cell line. Estrogen receptor beta plays a vital role in the anti-proliferative activity on the HT-29 cell line. Jaouen and co-workers synthesized ferrocenyl – steroid hybrid compounds and tested them for their anticancer activity in vitro against two human breast cancer cell lines MCF-7 and MDA-MB-231. They also reported the synthesis of steroid vectorized ferrocene derivatives and evaluated their antiproliferative effect against prostate cancer cells LNCaP and PC-3 with IC_{50} values ranging between 4.7

and 8.3 μM. At high concentrations (10 μM) the compounds exhibited good antiproliferative activity but poor or no activity at low concentrations (1 μM) against the cancer cells [44].

Herein we report the synthesis and characterization of the ferrocenyl thiosemicarbazones **L9-12**.

2.4.2 Materials and instrumentation:

The chemicals and solvents used in the experiment were all of analytical grade. Ferrocencarboxaldehyde was purchased from Acros organics, the thiosemicarbazide was purchased from SRL (Sisco research laboratory, Mumbai, India.). ^{1}H NMR spectra, Mass spectra, Infrared spectra, UV spectra and CHN were recorded on same instruments as mention in section 2.2.2.

2.4.3 Synthesis and characterization:

The ligands were synthesized and characterised according to the literature [45]. A solution of the appropriate thiosemicarbazide (1.0 mmol) in water (45 ml) was added drop wise to a hot, stirred solution of ferrocenecarboxaldehyde (1.0 mmol) in ethanol (35 ml). Acetic acid (1 ml) was added and the mixture was heated under reflux for 15 min and then stirred for a further 12 h. The resulting orange **(L1, L2)** or red **(L3, L4)** solid was filtered off and dried under vacuum. All the ligands were recrystallized from methanol and pure product was isolated from it. Solubility: MeOH, DMSO and DMF.

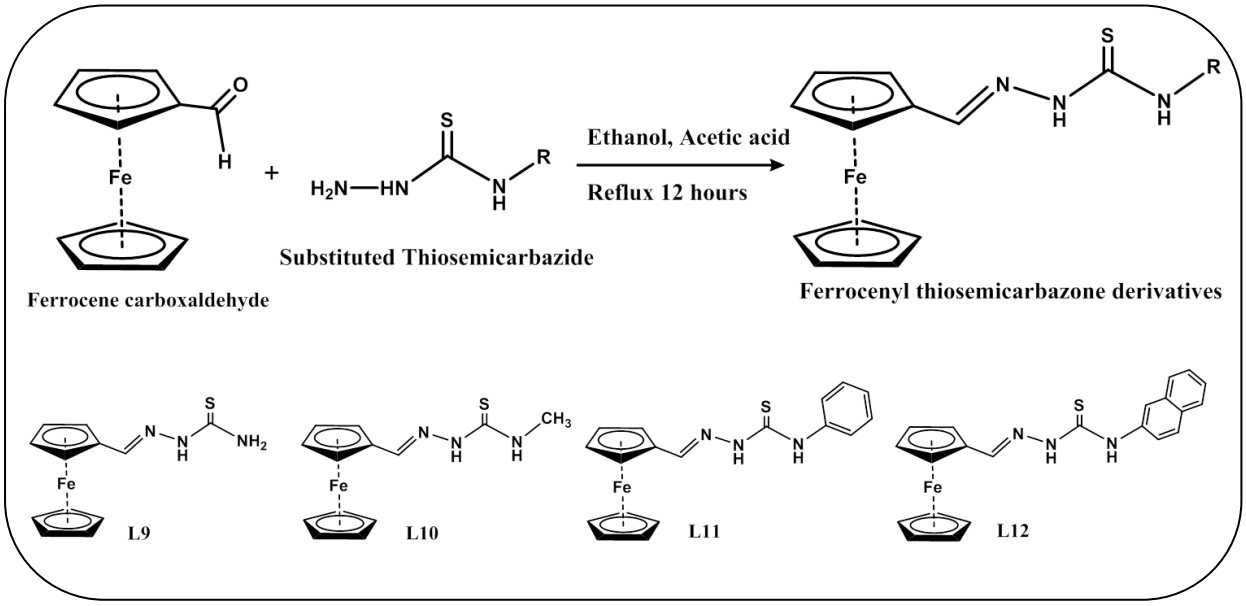

Fig 2.11: *General synthetic route to Ferrocenyl thiosemicarbazones* ***L9-12***

N-ferrocenyl-thiosemicarbazone ***(L9)***

L9 was synthesized by the condensation process of thiosemicarbazide (1.8 mmol, 170 mg) and ferrocenecarboxaldehyde (1.8 mmol, 400 mg). Yield 79.56 %; Molecular Weight 287.2 g/mol; Molecular Formula $C_{12}H_{13}FeN_3S$; Colour: orange; Anal. Found: C, 50.27; H, 4.30; N, 14.45. Calc.: C, 50.19; H, 4.56; N,14.63; MS (m/z) Obs (Calc): 287.9 (287.2) (M^+); ^{1}H-NMR (DMSO-d^6): δppm 4.81 (t, 2H, substituted cyclopentadiene); 4.71 (t, 2H, substituted cyclopentadiene); 4.18 (s, 5H, cyclopentadiene); 8.02-7.87 (s, 2H, NH_2); 7.60 (s, 1H, HC=N); 11.17 (s, 1H, N-NH); IR (KBr, cm^{-1}): *ν*(Ar)C-H 2975, *ν*(NNH) 3419; *ν*(NH_2) 3248; *ν*(C=N) 1587; *ν*(C=S) assym 1249; *ν*(C=S)sym 821.

N-ferrocenyl-4-methyl-3-thiosemicarbazone ***(L10)***

Condensation of 4-methyl-3-thiosemicarbazide (2.1 mmol, 230 mg) and ferrocenecarboxaldehyde (2.1 mmol, 468 mg) yielded **L10**. Yield 82.26 %; Molecular Weight 301.2 g/mol; Molecular Formula $C_{13}H_{15}FeN_3S$; Colour: orange; Anal. Found: C, 51.86; H, 4.96; N, 14.06. Calc.: C, 51.84; H, 5.02; N, 13.95 ; MS (m/z) Obs (Calc): 302.0 (301.2) (M^++1); ^{1}H-NMR (DMSO-d^6): δppm 4.40 (t, 2H, substituted cyclopentadiene); 4.72 (t, 2H, substituted cyclopentadiene), 4.19 (s, 5H, cyclopentadiene); 3.00, (s, 3H, N-CH_3); 7.87 (s, 1H, NH-CH_3); 8.17 (s, 1H, HC=N); 11.22 (s, 1H, N-NH); IR (KBr, cm^{-1}): ν(Ar)C-H 2995, *ν*(NN-H) 3345; *ν*(NH-CH_3) 3298; *ν*(C=N) 1608; *ν*(C=S) assym 1252; *ν*(C=S)sym 815.

N-ferrocenyl-4-phenyl-3-thiosemicarbazone ***(L11)***

L11 was prepared by condensation of 4-phenylthiosemicarbazide (1.1 mmol, 200 mg) and ferrocenecarboxaldehyde (1.1 mmol, 255 mg).Yield 71.08 %; Molecular Weight 363.3 g/mol; Molecular Formula $C_{18}H_{17}FeN_3S$; Colour: red; Anal. Found: C, 59.35; H, 4.53; N, 11.74. Calc.: C, 59.52; H, 4.72 ; N, 11.57; MS (m/z) Obs (Calc): 364.1 (363.3) (M^++1); ^{1}H-NMR (DMSO-d^6): δppm 4.45 (t, 2H, substituted cyclopentadiene),4.63 (t, 2H, substituted cyclopentadiene), 4.24 (s, 5H, cyclopentadiene); 7.26-7.69, (5H, m, N-C_6H_5); 9.10 (s, 1H, NH-C_6H_5); 7.86, (s, 1H, HC=N); 10.11, (s, 1H, N-NH); IR (KBr, cm^{-1}): ν(Ar)C-H 2882; *ν*(NN-H) 3343; *ν*(NH-C_6H_5) 3116; *ν*(C=N) 1598; *ν*(C=S)assym 1272; *ν*(C=S)sym 818.

N-ferrocenyl-4-(naphthalen-1-yl)-3-thiosemicarbazone ***(L12)***

Reaction of 4-(1-Naphthyl)-3-thiosemicarbazide (1.6 mmol, 360 mg) and ferrocenecarboxaldehyde (1.6 mmol, 354 mg) produced **L12**. Yield 75.5 %; Molecular Weight 413.3 g/mol; Molecular Formula $C_{22}H_{19}FeN_5S$; Colour: yellow; Anal. Found: C,

63.98; H, 4.61; N, 10.28. Calc.: C, 63.93; H, 4.63; N, 10.17; MS (m/z) Obs (Calc): 413.2 (413.3) (M^+); ^{1}H-NMR (DMSO-d^6): δppm 4.30 (t, 2H, substituted cyclopentadiene); 4.68 (t, 2H, substituted cyclopentadiene); 4.25 (s, 5H, cyclopentadiene); 7.52-7.89, (7H, m, N-$C_{10}H_7$); 10.90, (s, 1H, NH-$C_{10}H_7$); 8.05 (s, 1H, HC=N); 11.71, (s, 1H, N-NH); IR (KBr, cm^{-1}): *ν*(Ar)C-H 2964; *ν*(NN-H) 3344; *ν*(NH-$C_{10}H_7$) 3228; *ν*(C=N) 1598; *ν*(C=S)assym 1275; *ν*(C=S)sym 822.

2.4.4 Results and discussion:

The four ferrocenyl thiosemicarbazone derivatives have been synthesized according to the general synthetic route given in *Fig. 2.11* in good yields.

The UV spectra of the ligands **L9-L12** (*Fig. 2.12*) in MeOH was carried out in the region 200-600 nm. All the ligands show peaks in the range 227-228 nm, ascribed to the π→π* intra ligand transitions. Sharp but medium intensity *n*→π* bands at 305, 307, 314 and 321 nm for **L9**, **L10**, **L11** and **L12** respectively were observed, involving the molecular orbital of the cyclopentadienyl ring of ferrocene, C=N and enolic –SH chromophore. The shoulder observed in the region 459–464 nm in the ligands may be assigned to charge transfer transition from iron to either non-bonding or antibonding orbitals of the cyclopentadienyl ring, [46] which has been shown as an expansion in the inset of *Fig. 2.12*. The peak values have been tabulated in Table 2.5.

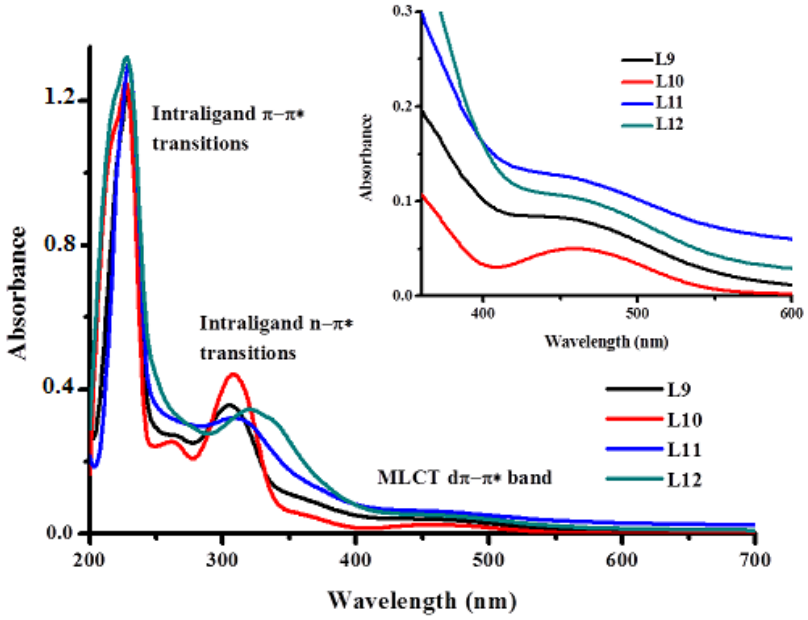

Fig. 2.12: *UV spectra of ligands* ***L9-12*** *recorded in MeOH with path length 1 cm.*

Table 2.5: UV peak assignments of **L9-12**

Code	L9	L10	L11	L12
Intra-ligand π-π* transitions(nm)	227	227	228	227
Intra-ligand n-π* transitions(nm)	305	307	314	321
Intra-ligand dπ(Fe^{2+})-n/π* transitions(nm)	459	462	461	464

The ESI-MS spectra of the ligands (*Fig. 2.13*) showed molecular ion peaks corresponding to M^+ species at m/z values 287.9, 302.0, 364.1 and 413.2 for **L9, L10, L11** and **L12** respectively which is in well agreement with the proposed composition. The m/z values have been tabulated in Table 2.6.

Table 2.6: m/z values of Ligands

Code	L9	L10	L11	L12
Calculated Mass (g/mol)	287.2	301.2	363.3	413.3
Observed Mass (g/mol)	287.9	302.0	364.1	413.2

The IR spectra of the ligands **L9-12** displayed characteristic strong stretching bands at 1587-1608 cm^{-1} due to (-CH=N-) present in ferrocenyl thiosemicarbazone derivatives while bands attributed to asymmetric and symmetric stretching of -C=S at 1249-1275 cm^{-1} and 815-822 cm^{-1} respectively are also observed. The other bands observed are due to –N-HR stretching at 3116-3248 cm^{-1}. The presence of weak to medium bands in the fingerprint regions 2882-2995 cm^{-1} are attributed to aromatic ν_{C-H} stretch of cyclopentadienyl rings and also to C_6H_5 (**L11**) and $C_{10}H_7$ (**L12**) groups.

The ^1H NMR spectra of the ligands **L9-12** (*Fig. 2.14*) exhibit 9 proton multiplet in the δ range of 4-5 ppm that can be ascribed to the ferrocenyl ring protons as mention in section 2.4.3. The major signals appeared in ^1H NMR spectra of the ligands are as follows, the

signals due to (-C**H**=N-) proton, present in these ligands at **L9** 7.60 ppm, **L10** 8.17 ppm, **L11** 7.86 ppm and **L12** 8.05 ppm as a singlet. The –N-N**H** protons were observed at 11.17ppm (**L9**), 11.22 ppm (**L10**), 10.11ppm (**L11**) and 11.71 ppm (**L12**) as a singlet and the singlets arising due to N**H**$_2$ in **L9** at 8.02, 7.87ppm, N**H**-CH_3 in **L10** at 7.87ppm, N**H**-C_6H_5 in **L11** at 9.10 ppm and N**H**-$C_{10}H_7$ in **L12** at 10.90 ppm confirm the formation of Schiff bases via condensation reaction between the thiosemicarbazides and ferrocenecarboxaldehyde. For ligands **L11** and **L12** the N**H**-C_6H_5 and N**H**-$C_{10}H_7$ protons are at 9.10 ppm and 10.90 ppm compared to 7.87 - 8.02 ppm observed for the others. This downfield shift is possibly due to the proton locating in the cone of the phenyl ring or more likely to the electron density redistribution in the skeleton of the molecule. For **L9**, the N**H**$_2$ group generates two distinct singlet at 8.02 and 7.87 ppm. This pattern is to be expected as the protons are magnetically non-equivalent as a consequence of the C−NH_2 bond possessing some π character via the mesomeric effect [47]. All the other protons due –CH_3 δ = 3 ppm, –C_6H_5 δ = 7.26 – 7.69 ppm and –$C_{10}H_7$ δ = 7.52 – 7.89 ppm, resonate in regions commonly as expected.

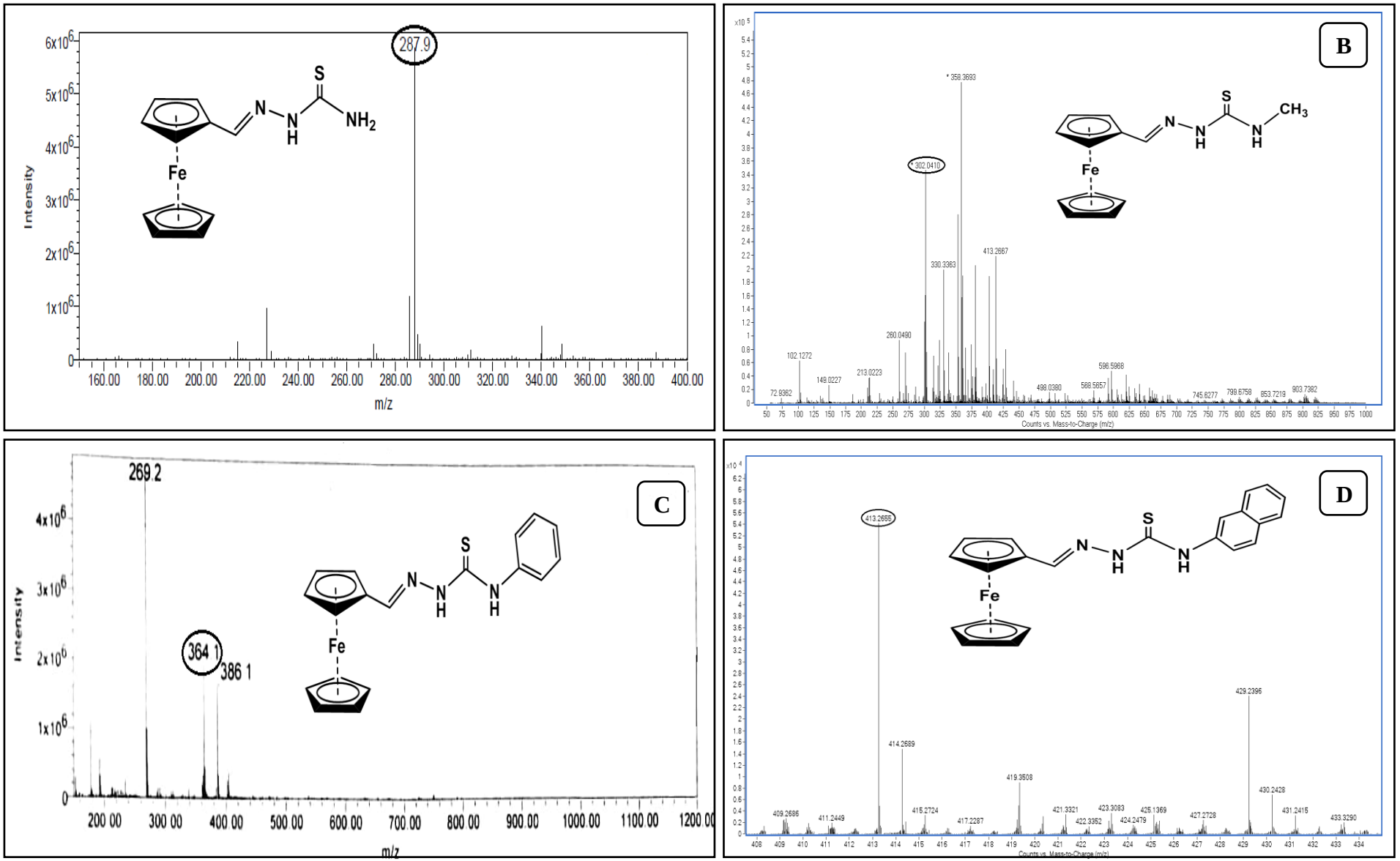

Fig. 2.13: *ESI-MS spectra of ligands (A)* ***L9*** *(B)* ***L10*** *(C)* ***L11*** *(D)* ***L12*** *indicating their molecular ion peak*

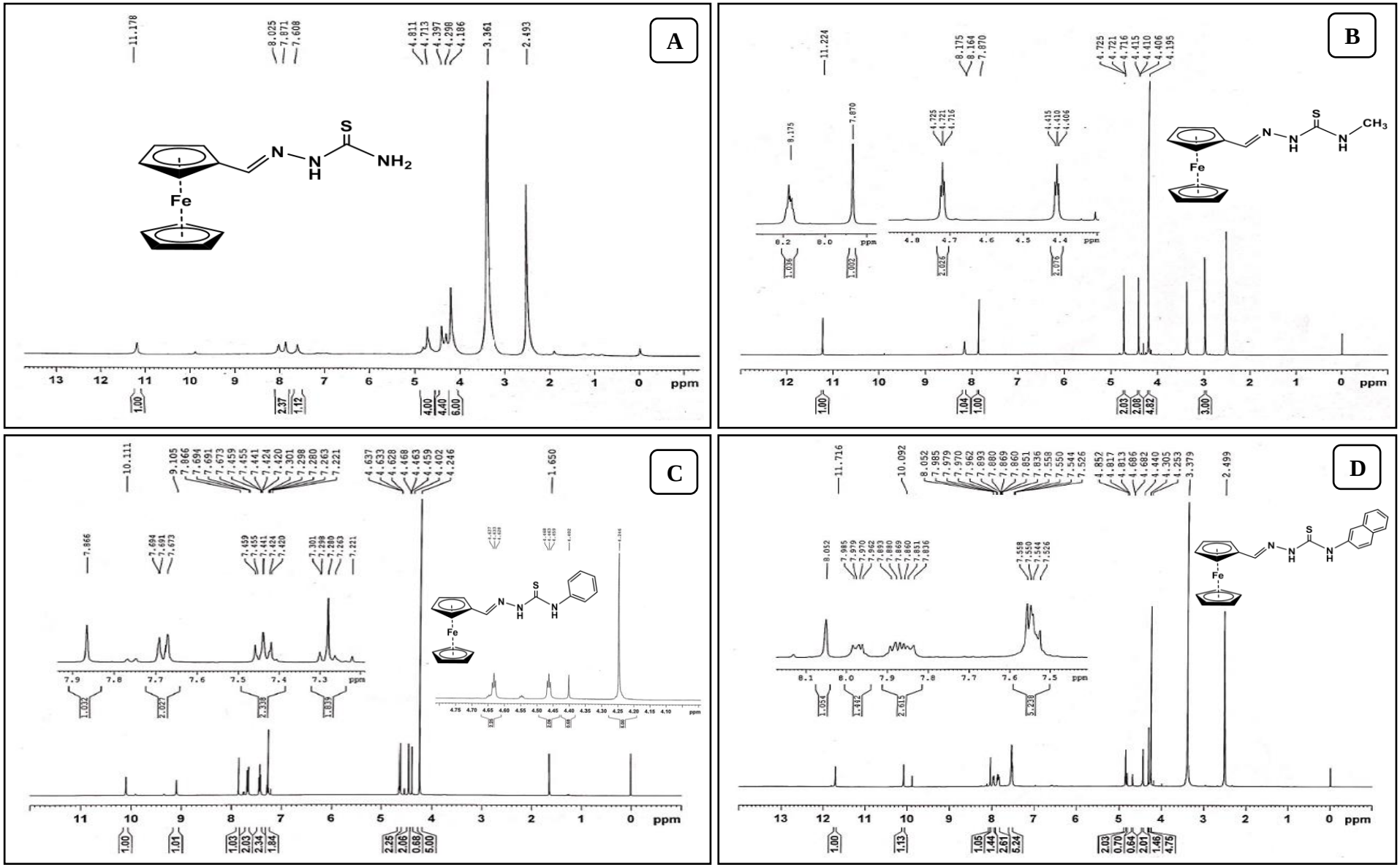

Fig. 2.14: *^{1}H NMR spectra of ligands (A)* ***L9*** *(B)* ***L10*** *(C)* ***L11*** *(D)* ***L12***

2.5 Ferrocene mannich bases (L13-L16):

2.5.1 Introduction:

Throughout the last decade, a large number of novel Mannich bases have been synthesized and evaluated as potential candidates for the treatment of a multitude of diseases and medical conditions, as prodrugs, or as molecules evoking a response from biological targets. The structure activity relationship studies for Mannich bases derived from structurally diverse substrates have allowed better insight into the design of more effective drug candidates in future. Immense progress has been made in the field of anticancer and antimicrobial agents, and medicinal chemists have witnessed the chemical modification of many biologically active, naturally-occurring substrates or well established drugs by means of the Mannich reaction with improved biological activity. As such, the Mannich reaction has been used extensively in medicinal chemistry, for the synthesis of novel chemical species endowed with various and interesting biological properties, and for the modification of physico-chemical properties of a candidate, that ultimately influence the candidate's bioavailability, performance and pharmacological activity as a drug. A detailed review entitled "Mannich bases in medicinal chemistry and drug design" by Gheorghe Roman gives an overview of the potential of Mannich bases as anticancer and cytotxic agents along with other medicinal applications of these compounds [48].

Herein we report the synthesis of ferrocene conjugated amino acid Mannich bases [**L13 - L16**]

2.5.2 Materials and instrumentation:

All the chemicals and solvents purchased are of analytical grade. Elemental and spectral analysis was performed on the same instrument models as mentioned previously (section 2.2.2).

2.5.3 Synthesis and characterization:

The ferrocenyl amino acids were synthesized according to a procedure reported by Chakravarty *et al* [49]. Amino acid (2.76 mmol) and NaOH (2.76 mmol) in dry methanol (5 ml) were stirred for 30 min to get a homogeneous solution. A methanolic solution (5 ml) of ferrocene carboxaldehyde (2.76 mmol) was added dropwise to the above solution, which was refluxed for 90 min, cooled, and treated with sodium borohydride (5.2 mmol) with constant

stirring. The solvent was evaporated, the resulting mass was dissolved in water and acidified with dilute HCl, and the solution pH was maintained within 5-6. The ligand that precipitated as a yellow solid was filtered, thoroughly washed with water and cold methanol, and finally dried in vacuum (*Fig. 2.15*). Yields of all the four ligands were in the range of 70-80 %.

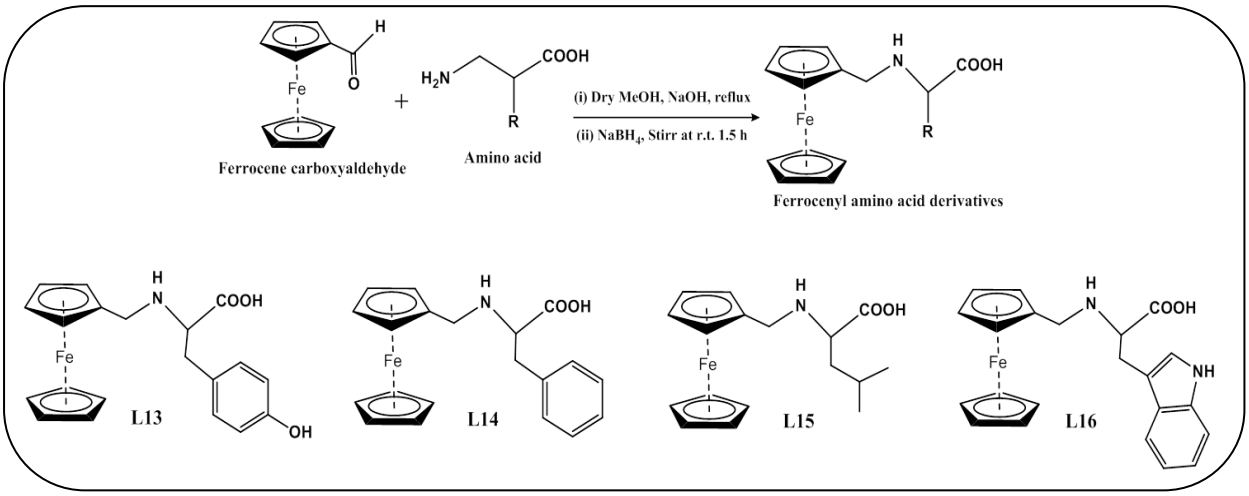

Fig 2.15: *General synthetic route to Ferrocenyl Mannich bases* ***L13-16***

2.5.4 Results and discussion:

All the Ferrocenyl amino acids ligands **L13-16** were synthesized by the above mention procedure and characterized by various spectral techniques to confirm their compositions as reported in literature [50].

2.6 Fluoroquinolones (L17-L20):

2.6.1 Introduction:

Despite being discovered serendipitously, the fluoroquinolones (FQs) are presently the largest class of antimicrobial agents used worldwide. Nalidixic acid the first quinolone recognized to exhibit antibacterial activity was isolated as a by-product during chloroquine synthesis in 1962. Over the next few years, extensive research led to discovery of the first generation of quinolones that overcame the limitations of parent molecule such as poor bioavailability and specificity only to gram-negative bacteria [51]. Later it was discovered that few structural modifications in the generic 4-quinolone backbone or its functional groups leads to enhanced bacterial cell penetration and prominent DNA gyrase inhibitory effect [52]. The quinolones are thus classified into four generations on the basis of their pharmacokinetic profile and antimicrobial activity (*Fig. 2.16*). A fluorine atom at C-6 position and cyclic

diamine piperazine molecule at C-7 position yielded the present-day FQs that possess significant potential against gramnegative, gram-positive and anaerobic bacteria. Fluoroquinolones (FQs) are well known to inhibit replication and transcription of bacterial DNA either by targeting DNA gyrase or by targeting topoisomerase-II, both the enzymes being imperative in bacterial growth.

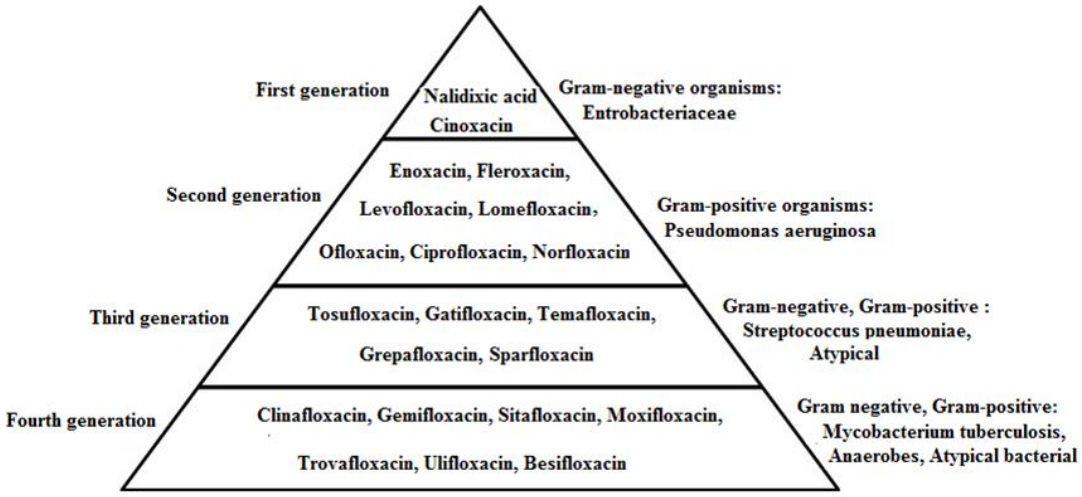

Fig. 2.16: *Classification of fluoroquinolones into four generations*

Reports have suggested that fluoroquinolones possess anticancer potential which is revealed by their ability to induce apoptosis and cancer associated-microRNA biogenesis, inhibit cell cycle progression by inducing cell cycle arrest and inhibit EMT (Epithelial-Mesenchymal-Transition). They are also known to regulate cancer stemness (*Fig. 2.17*) [53].

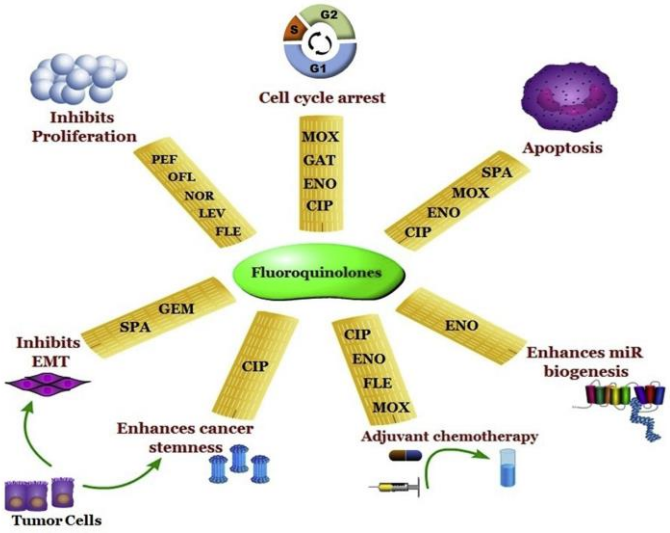

Fig. 2.17: *Anticancer activities of the fluroquinolones [54]*

Thus the remarkable efficiency of FQs to inhibit cancer cell growth in vitro and in vivo has rendered them as dual-purpose drugs. For instance, inception of ciprofloxacin into the clinical trials for bladder cancer and acute myeloid leukaemia treatment have amalgamated the demand for them to be looked upon as a probable candidate for drug repositioning from antibiotics to anticancer [54]

Looking at these antibacterial and anticancer activities of the fluoroquinolones as mentioned above, we have incorporated four different fluoroquinolones: Lemofloxacin (**L17**), Levofloxacin (**L18**), Ciprofloxacin (**L19**) and Moxifloxacin **(L20)** (*Fig. 2.18*) into our study. The fluoroquinolones were procured as generous gifts from local pharmaceutical companies with 99% HPLC purity.

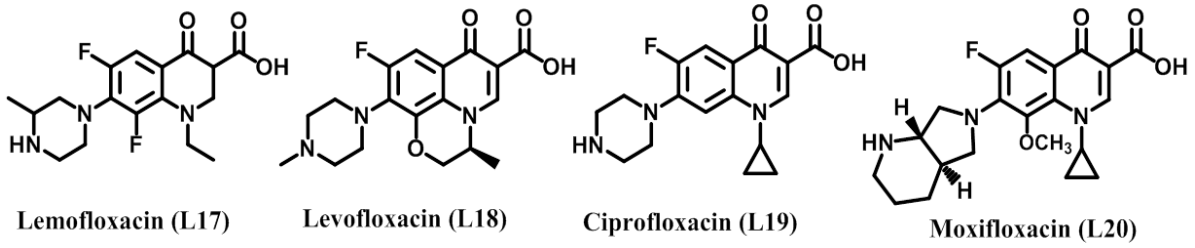

Fig. 2.18: *Structures of the fluoroquinolones employed in the present study*

2.7 Summary:

The four different ligand series discussed in this chapter have been synthesized and well characterized with an aim to employ these organic bioactive ligands in the synthesis of binuclear Ru (II) arene complexes and check their bioactivities.

2.8 Reference:

[1] Jampilek, J. *Molecules*., **2019**, 24, 3839.

[2] El Sayed, M.T.; Hamdy, N.; Osman, D.; Ahmed, K.M. *Adv. Mod Oncol Res*., **2015**, 1, 20.

[3] Roder, C.; Thomson, M. *Drugs in R&D*., **2015**, 15, 13.

[4] Bosco, B.; Defant, A.; Messina, A.; Incitti, T.; Sighel, D.; Bozza, A.; Ciribilli, Y.; Inga, A.; Casarosa, S.; Mancini, I. *Molecules.*, **2018**, 23, 1996.

[5] Wang, W.; Lei, L.; Liu, Z.; Wang, H.; Meng, Q. *Molecules*., **2019**, *24*, 877.

[6] Ansari, A.; Ali, A.; Asif, M.; Shamsuzzaman. *New J. Chem.*, **2017**, 41, 16.

[7] Huang, Y. Y.; Wang, L. Y.; Chang, C. H.; Kuo, Y. H.; Wong, F. F. *Tetrahedron.*, **2012**, 68, 9658.

[8] Mert, S.; Yağlıoğlu, A. S.; Demirtas, I.; Kasımoğulları, R. *Med. Chem. Res.*, **2014**, 23, 1278.

[9] Via, L.D.; Marini, A.M.; Salerno, S.; Motta, C. L.; Toninello, A. *Bioorg. Med. Chem.*, **2009**, 17, 326.

[10] Li, D.; Shu, Y.; Li, P.; Zhang, W.; Ni, H.; Cao, Y. *Med. Chem. Res.*, **2013**, 22, 3109.

[11] Nitulescu, G. M.; Draghici, C.; Missir, A. V. *Eur. J. Med.Chem.*, **2010**, 45, 4914.

[12] Prasad, Y.R.; Kumar, G.V.S.; Chandrashekar, S.M. *Med. Chem. Res*., **2013**, 22, 2061.

[13] Rai, U.S.; Isloor, A.M.; Shetty, P.; Pai, K.S.R.; Fun, H.K. *Arabian J. Chem.*, **2015**, 8, 317.

[14] Saleh, N.M.; El-Gazzar, M. G.; Aly, H. M.; Othman, R. A. *Front. Chem.*, **2020**, 7, 917.

[15] Karrouchi, K.; Radi, S.; Ramli, Y.; Taoufik, J.; Mabkhot, Y. N.; Al-aizari, F. A.; Ansar, M. *Molecule*s, **2018**, 23, 134.

[16] Prajapati, N. P.; Patel, H. D. *Synth. Commun.*, **2019**,49, 2767.

[17] Dömötör, O.; Kiss, M.A.; Gál, G.T.; May, N.V.; Spengler, G.; Nové, M.; Gašparović, A. C.; Frank, E.; Enyedy, E.A. *J. Inorg. Biochem.*, **2020**, 202, 110883.

[18] Sirbu, A.; Palamarciuc, O.; Babak, M.V.; Lim, J. M.; Ohui, K.; Enyedy, E. A.; Shova, D.S.; Darvasiová, D.; Rapta, P.; Ang, W. H.; Arion, V.B. *Dalton Trans.*, **2017**, 46, 3833.

[19] Patel, H.D.; Divatia, S.M.; Clercq, E.D. *Ind. J. of Chem.*, **2013**, 52, 535.

[20] Sampath, K.; Krishnan, C. J. *Arab. J. Chem.*, **2017**, 10, S3207.

[21] Yousef, T. A.; El-Reash, G. M. A. *J. Mol Struct*., **2020**, 1201, 127180.

[22] Kumar, V.;Mudgal, M.M.; Rani, N.;Jha, A.; Jaggi, M.; Singh, A. T.;Sanna, V. K.; Singh, P.; Sharma, P. K.; Irchhaiya, R.; Burman, A.C. *J. Enzym. Inh. Med. Chem*., **2009**, 24, 763.

[23] Sidoryk, K.; Świtalska, M.; Wietrzyk, J.; Jaromin, A.; Piętka-Ottlik, M.; Cmoch, P.; Zagrodzka, J.; Szczepek, W.; Kaczmarek, L.; Peczyńska-Czoch, W. *J. Med. Chem.*, **2012**, 55, 5077.

[24] Ali, I.; Wani, W. A.; Haque, A.; Saleem, K. *Future Med. Chem.*, **2013**, 5, 961.

[25]Rupar, J.; Dobričić, V.; Grahovac, J.; Radulovi, S.; Skok, Z .; Ilaš, J.; Aleksić, M.; Brborić, J.; Čudina, O. *RSC Med. Chem.*, **2020**, 11, 378.

[26] De Castro, P. P.; Siqueira, R. P.; Conforte, L.; Franco, C. H.J.; Bressan, G.C.; Amarante, G.W. *J. Braz. Chem. Soc.*, **2020**, 31, 193.

[27]Joksovic´, M. D.; Bogdanovic´, G.; Kojic´, V.; Me´sza´ros, K.; Sze´cse´nyi, Leovac, M.V.; Jakimov, D.; Trifunovic´, S.; Markovic´, V.; Joksovic´ L. *J. Heterocyclic Chem.*, **2010**, 47, 850.

[28] Grumezescu, A. Elsevier; Johannesburg, South Africa, **2017**, 33.

[29] Peter, S.; Aderibigbe, B.A. *Molecules*, **2019**, 24, 3604.

[30] Quirante, J.; Dubar, F.; González, A.; Lopez, C.; Cascante, M.; Cortés, R.; Forfar, I.; Pradines, B.; Biot, C. *J. Organomet. Chem.*, **2011**, 696, 1011.

[31] Reiter, C.; Karagöz, A.C.; Fröhlich, T.; Klein, V.; Zeino, M.; Viertel, K.; Held, J.; Mordmüller, B.; Öztürk, S.E.; Anıl, H.; Efferth, T.; Tsogoeva, S.B. *Eur. J. Med. Chem.* **2014**, 75, 403.

[32] Wang, Y.; Dansette, P.M.; Pigeon, P.; Top, S.; McGlinchey, M.J.; Mansuy, D.; Jaouen, G. *Chem. Sci.*, **2017**, 9, 70.

[33] (a) Wang, Y.; Pigeon, P.; McGlinchey, M. J.; Top, S.; Jaouen, G. *J. Organomet.Chem.* **2017**, 829, 108. (b) Pigeon, P.; Wang, Y.; Top, S.; Najlaoui, F.; Alvarez, M. C. G.; Bignon, J.; McGlinchey, M.J.; Jaouen, G. *J. Med. Chem.*, **2017**, 60, 8358.

[34] Vessières, A.; Top, S.; Pigeon, P.; Hillard, E.; Boubeker, L.; Spera, D.; Jaouen, G. *J. Med. Chem.*, **2005**, 48, 3937.

[35] Plażuk, D.; Rychlik, B.; Błauz, A.; Domagała, S. *J. Organomet. Chem.*, **2012**, 715, 102.

[36] Pedotti, S.; Ussia, M.; Patti, A.; Musso, N.; Barresi, V.; Condorelli, D. F. *J. Organomet. Chem.*, **2017**, 830, 56.

[37] Panaka, S.; Trivedi, R.; Jaipal, K.; Giribabu, L.; Sujitha, P.; Kumar, C. G.; Sridhar, B. *J. Organomet. Chem.* **2016**, 813, 125.

[38] De Oliveira, A.C.; Hillard, E.A.; Pigeon, P.; Rocha, D.D.; Rodrigues, F.A.; Montenegro, R.C.; Costa-Lotufo, L.V.; Goulart, M.O.; Jaouen, G. *Eur. J.Med. Chem.*, **2011**, 46, 3778.

[39] Jadhav, J.; Juvekar, A.; Kurane, R.; Khanapure, S.; Salunkhe, R.; Rashinkar, G. *Eur. J. Med. Chem.*, **2013**, 65, 232–239.

[40] Pérez, W.I.; Soto, Y.; Ortíz, C.; Matta, J.; Meléndez, E. *Bioorg.Med.Chem.*, **2015**, 23, 471.

[41] Vera, J.L.; Rullán, J.; Santos, N.; Jiménez, J.; Rivera, J.; Santana, A.; Briggs, J.; Rheingold, A. L.; Matta, J.; Meléndez, E. *J. Organomet. Chem.*, **2014**,749, 204.

[42] Hussain, R.A.; Badshah, A.; Pezzuto, J.M.; Ahmed, N.; Kondratyuk, T.P.; Park, E.J. *J. Photochem. Photobio*., **2015**, 148, 197.

[43] Narváez-Pita, X.; Rheingold, A.L.; Meléndez, E. *J. Organomet. Chem*., **2017**, 846, 113.

[44] Jaouen, G.; Vessières, A.; Top, S. *Chem. Soc. Rev.*, **2015**, 44, 8802.

[45] Casas, J. S.; Castaño, M.V.; Cifuentes, M.C.; Monteagudo, J.C.G.; Sánchez, A.; Sordo, J.; Abram, U. *J. Inorg. Biochem.*, **2004**, 98, 1009.

[46] Prabhakaran, R.; Anantharaman, S.; Thilagavathi, M.; Kaveri, M.V.; Kalaivani, P.; Karvembu, R.; Dharmaraj, N.; Bertagnolli, H.; Dallemer, F.; Natarajan, K. *Spectrochim. Acta*. **2011**, 78, 844.

[47] Beckford, F.; Dourth, D.; ShaloskiJr, M.; Didion, J.; Thessing, J.; Woods, J.; Crowell, V.; Gerasimchuk, N.; Gonzalez-Sarrías, A.; Seeram, N. P. *J. Inorg. Biochem.*, **2011**, 105, 1019.

[48] Roman, G. *Eur. J. Med. Chem*., **2015**, 89, 743.

[49] Ramadevi, P.; Singh, R.; Jana, S.S.; Devkar, R.; Chakraborty, D. *J. Organomet. Chem.* **2017**, 833, 80.

[50] Ramadevi, P.; Singh, R.; Jana, S.S.; Devkar, R.; Chakraborty, D. *J. Photochem. Photobiol. A: Chem.* **2015**, 305, 1.

[51] Andersson, M. I.; MacGowan, A. P. *J. Antimicrob. Chemother.*, (Suppl 1) **2003**, 51, 1.

[52] Aldred, K. J.; Kerns, R. J.; Osheroff, N. *Biochem*. **2014**, 53, 1565.

[53] Yadav, V.; Talwar, P.; *Biomed. Pharmacother*., **2019**, 111, 934.